Synthesis – properties correlation and the unexpected role of the titania support on the Grignard surface modification

Synthesis – properties correlation and the unexpected role of the titania support on the Grignard surface modification

Jeroen G. Van Dijck [a,b], Pieter Mampuys [c], H.Y. Vincent Ching [d], Dileep Krishnan [e], Kitty Baert [f], Tom Hauffman [f], Johan Verbeeck [e], Sabine Van Doorslaer [d], Bert U.W. Maes [c], Matthieu Dorbec [b,1], Anita Buekenhoudt [b], Vera Meynen [a*]

[a] Laboratory for Adsorption and Catalysis (LADCA), Department of Chemistry, University of Antwerp, Universiteitsplein 1, 2610, Wilrijk, Belgium, jeroen.vandijck@uantwerpen.be, vera.meynen@uantwerpen.be

[b] VITO NV - Flemish Institute for Technological Research NV, Separation and Conversion Technologies, Boeretang 200, 2400, Mol, Belgium, jeroen.vandijck@vito.be, anita.buekenhoudt@vito.be

[c] Organic Synthesis, Department of Chemistry, University of Antwerp, Groenenborgerlaan 171, 2020 Antwerp, Belgium, pieter.mampuys@uantwerpen.be, bert.maes@uantwerpen.be

[d] BIMEF Laboratory, Department of Chemistry, University of Antwerp, Universiteitsplein 1, 2610, Wilrijk, Belgium, HongYueVincent.Ching@uantwerpen.be, sabine.vandoorslaer@uantwerpen.be

[e] EMAT, Department of Physics, University of Antwerp, Groenenborgerlaan 171, 2020 Antwerp, Belgium, dileep.krishnan@uantwerpen.be ,jo.verbeeck@uantwerpen.be

[f] Res. Dept. Electrochemical & Surface Engineering, Department of Materials and Chemistry, Vrije Universiteit Brussel, Pleinlaan 2, 1050 Brussels, Belgium, kitty.baert@vub.be, tom.hauffman@vub.be

*corresponding author: Laboratory for Adsorption and Catalysis (LADCA), Department of Chemistry, University of Antwerp, Universiteitsplein 1, 2610, Wilrijk, Belgium, vera.meynen@uantwerpen.be, +3232652368

[1]Present address: API Small Molecule - Chemical Process Development, Janssen Pharmaceutica NV, Turnhoutseweg 30, 2340 Beerse, Belgium, MDorbec@ITS.JNJ.com

ABSTRACT

While the impact of reaction conditions on surface modification with Grignard reactants has been studied for silica supports, such information is absent for metal oxide supports such as titania. Differences between modified/functionalized titania and silica are observed, making it paramount to explore the reaction mechanism. A detailed study on the impact of the reaction conditions is reported here, with a specific focus on the chain length of the alkyl Grignard reactant, the reactant concentration, the reaction time and temperature, and the type of titania support. While the increase in the chain length reduces the amount of organic groups attached to the surface, the concentration, time and temperature show little to no influence on the modification degree. However, the type of titania support used and the percentage of amorphous phase present in the support material has a significant impact on the amount of surface grafted groups. Even though the temperature and concentration show no clear impact on the modification degree, it is clearly observed that they can cause changes in the surface hydroxyl population. It is further shown that these changes are not linked to the modification degree. During functionalization, the titania support is reduced as well. This reduction is dependent on the reaction temperature, the titania support and the chain length of the Grignard reactant. Just as for the changes in the surface hydroxyl population, the influence on the reduction is not linked to the modification degree.

Keywords: Titanium dioxide, Grignard reactants, Surface modification, Synthesis - properties correlation

1. Introduction

Partly due to their robustness, metal oxide supports are of great interest for industrial applications such as membranes,[1,2] solar cells,[3] implants[4] and catalysts[5] to name a few. Unfortunately, for several applications such as sorption and separation, their use is limited, due to their hydrophilic surface limiting the type of interaction they may have. A way to overcome this problem is grafting the metal oxide supports with organic groups. This

allows the introduction of specific interactions, increasing their applicability and performance.

Different precursor molecules can be used to graft the surface: alcohols[6–8], organosilanes[9–14], organophosphonic acids or their derivatives[15–21] and others[6] have all shown their ability to form functional organic (mono)layers onto the oxide surface. While these methods have their specific advantages, all bonds occur through heteroatoms (*e.g.* O, Si or P). These heteroatoms can pose stability issues[16] or introduce (unwanted) side interactions besides the intended interaction of the organic group.[22–25] Having a direct bond between the surface and the organic group (M-R) can prevent these unwanted interactions, providing unique behavior in application.[2,23,25–29] This can be achieved by using organometallic reactants.

The first use of organometallic reactants (organomagnesium halide and organolithium) to modify an oxide surface, in this case silica, was reported by Duel *et al.*[30] The formation of Si-R bonds was confirmed by infrared spectroscopy. Later, a *one-pot* reaction between ordered mesoporous silica and organometallic reactants was reported independently by Lim *et al.*[31] and Bein *et al.*[32–36] They found that the Si-R bonds are formed by a direct attack of the organometallic reactant at the silicon atom of a siloxane bridge. Bein *et al.*[34] further investigated how to optimize the reaction conditions to find the most efficient and economic conditions for the desired organic surface modification. They found that the degree of surface substitution can be controlled within a broad range up to very high levels (from < 1 mmol g^{-1} up to 5 mmol g^{-1}) by varying the concentration of the organometallic reactant, reaction temperature or reaction time. However, they observed a strong decrease in structural order of the support when modifying with the highest concentration, temperature and reaction time due to the increase in siloxane bridge breaking.

Besides silica, other supports have also been modified using organometallic reactants. Müller *et al.* modified tin oxide.[37] While the same mechanism as for silica was assumed, no experimental proof was provided. Furthermore, no study was performed to evaluate the impact of the reaction conditions on the modification. In addition porous silicon has been modified by Kim *et al.*[38,39] and Song *et al.*[40] They demonstrated that the mechanism proceeds through the breakage of a Si-Si bond, forming Si-R and Si-Li or Si-MgX bonds on the surface. The Si-Li/MgX bond is reactive enough to act as a center for other modification methods (such as organosilation). When modifying a non-porous silicon wafer Wayner *et al.*[41,42] found that the Si-Si bond was not cleaved but instead all Si-H bonds were consumed during the reaction. They speculated that the breaking of a Si-Si bond on the surface of the wafer would introduce too much strain to be stable. This indicates that besides reaction parameters, the surface itself might greatly influence the modification and/or its mechanism.

Transition metal oxides like titania have also been modified.[2,23–27,43,44] Meynen *et al.*[44] presented the successful grafting of *n*-alkyl groups onto the surface of titania as well as the main characteristics of the grafted materials. However, no mechanism was proposed, but some insights were given. A color change during the reaction was reported and assumed to be caused by the transition from Ti(IV) to Ti(III) , as was reported for black titania produced *via* other methods,[45–48] but no experimental proof was provided. The mechanism therefore seemed to be more complex than a simple nucleophilic attack on the titanium surface and subsequent M–O bond cleavage, as it has been suggested for silica. Also the behavior of this modified material in different applications[2,23,25–29] is significantly different when compared to other modification methods, even though the organic moiety is the same[23–25].

Since differences in the modification of titania with Grignard reactants are observed and changes in the support properties became visible (*e.g.* titania reduction), in contrast to the reported modification of silica[30–36], questions are raised on whether the impact of the different reaction conditions on the resulting modified material properties are the same as those reported for silica. Moreover, it is interesting to evaluate whether the more diverse structural properties of the titania support material, *i.e.* crystal phases and amorphous content, plays a role.

We report here a detailed study of the impact of the reaction conditions on the Grignard grafting of TiO_2. The reaction conditions investigated are the reaction temperature, the reaction time, the concentration of the Grignard reactant and the chain length of the Grignard reactants, in order to elucidate the synthesis–properties correlation and provide insights in the reaction mechanism. Furthermore, any influences of the titania support properties on the modified materials properties are also evaluated.

2. Experimental Section

2.1. Titania supports

Different titania supports have been studied: the commercially available P25 (Evonik), a sol-gel synthesized titania (denoted as $sTiO_2$) - obtained by using the same colloidal sol as described by Van Gestel *et al.*[49] but instead of using the sol to dipcoat, it was poured in a Teflon dish and calcined at 470 °C for 3 h after evaporation of the solvent. Further, the commercial CristalACTIV^{TM} PC500 (Cristal) is applied after being calcined at 470 °C for 3 h (denoted as PC500) and a variety of mesoporous titania materials synthesized by using an adapted method from the reported dual template synthesis.[50] The synthesis for these mesoporous titania was altered by adding an acid solution (1mL), such as HCl (0.1M), H_2SO_4 (0.01M), H_2SO_4 (0.1M) or H_2SO_4 (1M), to the final reaction mixture after 2 h. The addition of the acid solution give more narrow and controllable pore size distributions. Full synthesis

and characterization of the materials was reported by S. Loreto *et al.*[51] These supports are denoted as TiO_2 HCl, TiO_2 H_2SO_4-0.01, TiO_2 H_2SO_4-0.1 or TiO_2 H_2SO_4-1 depending on the acid and its concentration used during synthesis.

Titania support	P25	PC500	TiO_2 HCl	TiO_2 H_2SO_4-1	TiO_2 H_2SO_4-0.1	TiO_2 H_2SO_4-0.01	sTiO_2
Crystal phase*	Anatase + Rutile	Anatase	Anatase	Anatase + Rutile	Anatase	Anatase	Anatase +brookite
Surface area (m^2/g)**	50-55	100	140	140	130	140	100
D_p BJH des (nm)**	n.a.	6.6	9.6	17	9.8	9.8	7.9

*Table 1: Characteristics of used titania supports. *As determined by EELS, **As determined by N_2 sorption*

A summary of all the characteristics of the different titania can be found in Table 1. Nitrogen sorption isotherms and pore size distributions are shown in Appendix A Figure A.1.A

2.2. Characterization of the support materials

Electron energy loss spectrum (EELS) images were acquired in STEM mode using an aberration corrected FEI Titan 60-300 kV transmission electron microscope operating at an acceleration voltage of 120 kV. An angstrom-sized probe with electron probe current of 50 pA was used. A dwell time of 0.5 s/pixel was used for spectrum image acquisition. The monochromator was excited to ensure that the energy resolution was as good as 100 meV. The spectra thus obtained were fit with a power-law background along with normalized spectra obtained from reference samples of anatase (Merck, ref 232033), rutile (Merck, ref 224227), brookite (Merck, ref 791326) and amorphous (phosphonic acid modified) titaniaphosphonate for quantification using EELS model software[52].

The amorphous powder sample, applied in the EELS measurements, was prepared by adding titaniumisopropoxide (0.01 mol, Sigma-Aldrich) in ethanol (5.7 mL) dropwise to a solution of phenylphosphonic acid (0.02 mol, Sigma-Aldrich) in ethanol (5.0 mL), water (2.06 mL) and HCl (1.18 mL, 36%) with hexadecyltrimethylammonium bromide (0.59 g, 1.6 mmol, CTAB). After the formation of a white turbid solution, ethanol (10 mL) was added to decrease the viscosity and improve the stirring of the mixture. After 15 min of stirring, the mixture was transferred to a Petri dish and aged at 60 °C for 7 days. Raman spectroscopy was used to confirm the absence of crystal phases in the reference materials. The spectra can be found in Figure A.2 in Appendix A.

All Raman measurements were done using a HORIBA XploRA PLUS Raman microscope under the same conditions. A 532 nm diode-pumped solid-state (DPSS) laser with a power of 25 mW and a 10% filter was used for excitation and all the spectra were collected with an accumulation time of 15 s.

Nitrogen sorption measurements were recorded at -196 °C on a Quantachrome Quadrasorb SI automated gas sorption system. Before the measurements, the samples were degassed for 16 h under high vacuum at a temperature of 190 °C.

2.3. Grignard surface modification

Details of the modification procedure can be found in.[43] The modification protocol mentioned in [43] was used as follows: titania powder (1 g) was vacuum dried (10^{-4} mbar) at 190 °C for 16 h. The dried powder was cycled under vacuum into a glovebox (Argon atmosphere) and transferred in a dried glass bottle (150 °C for 16 h). Dry THF (30 mL, Merck, product: 186562) and 2 mmol of Grignard reactant [ethylmagnesium bromide (Merck, product: 364673) or propylmagnesium chloride (Merck, product: 224391) or octylmagnesium chloride (Merck, product 324566)] was added and the mixture was stirred for 72 h at room temperature (RT), unless mentioned otherwise. After stirring, the mixture

was filtered and washed over a paper filter with THF (3 x 30 mL) under inert atmosphere. The modified titania was transferred out of the glovebox and the mixture was washed with acetic acid (0.1 M, 3 x 30 mL) and finally stirred overnight in hot water at 70 °C under ambient atmosphere. The samples were further dried at 60 °C under vacuum (10^{-4} mbar). A blank modification with a sample that underwent the same synthesis steps without adding the Grignard reactant was performed as well.

To study the impact of different reaction conditions, some changes were made to the above mentioned basic modification protocol. When studying the concentration of the Grignard reactant: 2, 3, 4 or 6 mmol of octylmagnesium chloride (Merck, product 324566)] was evaluated. The impact of the reaction temperature was studied at -78 °C, RT and 65 °C. For these experiments the titania was added to a flame dried Kjeldahl flask (250 mL), equipped with a septum and a glass stirrer, inside the glovebox. After transferring out of the glovebox, the Kjeldahl flask was hooked up to a Schlenk line to ensure an inert atmosphere. For the experiments at 65 °C the Kjeldahl flask was equipped with an oven dried reflux condenser. The reaction mixtures were stirred at the indicated temperatures (in cooling or pre-heated oil bath) for both 4 h and 24 h. Since keeping the reaction mixture at -78 °C for 24 h was not possible due to practical reasons, a temperature of -78 °C was only maintained during the first 6 h and then the reaction mixture was allowed to warm up very slowly to RT, until a total reaction time of 24 h had been reached. To study the impact of the reaction time, experiments were performed for 4 h, 24 h, 48 h and 72 h. All these experiments have been performed on the P25 and $sTiO_2$ supports.

2.4. Determining the remaining percentage of Grignard reactant

Two methods were used to determine the remaining Grignard reactant: 1) titration and 2) deuterated octane quantification using GC-MS after quenching with D_2O.

The titration method is based on the method reported by Krasovskiy and Knochel[53] and follows the reaction procedure described below performed in a glovebox under argon atmosphere.

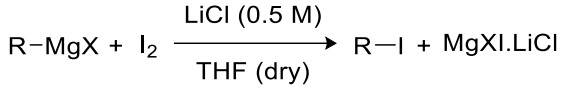

An aliquot (1 mL) of the reaction solvent was taken after 24 h, prior to the work-up of the modified titania using a syringe. It could not be avoided that some powder of the modified sample was present. An iodine solution (I_2, 0.067 M in THF (dry), Sigma-Aldrich), saturated with LiCl (Sigma-Aldrich, 0.5 M) was prepared. This iodine solution was added dropwise to the aliquot, *via* a graduated (1000 µL ± 50 µL) syringe until a slight yellow color was observed. This color change indicates that all remaining Grignard reactant has been consumed by I_2 and the endpoint of the titration has been reached. Based on the amount of iodine consumed, the remaining Grignard reactant can be calculated. All titrations have been repeated three times and an average value over three measurements has been used, all within a two percentage experimental error.

For the GC-MS method, the reaction mixture (still containing the modified titania) is quenched with D_2O (2 mL) prior to the work-up in order to ensure that all remaining octylmagnesium chloride is converted into octane. After stirring for 10 minutes at room temperature, the solid was allowed to settle down and an aliquot of 500 µL was taken via an Eppendorf pipet. 1,3,5-Trimethoxybenzene [500µL, 0.4 M in THF (dry)] was added as internal standard to the GC vial containing the quenched reaction mixture. This mixture was subsequently filtered using a CHROMAFIL® PET-20/25 syringe filter and diluted 100 times with THF. This sample was then analyzed by Gas Chromatography - Mass Spectrometry (GC-MS). 3 µL of the sample was injected. The apparatus used was an Agilent Technologies 7890 A GC System coupled to an Agilent Technologies 5975 C inert MSD with triple-axis

detector. As column an Optima 725820.30 30 m × 250 µm × 0.25 µm was selected. Carrier gas was helium. Inlet temperature heater: 225 °C. Oven program: 70 °C for 3 min, then heating 5 °C min^{-1} to 160 °C and heating at 160 °C for 2 min. A one minute post-run at 280 °C ends the oven program.

2.5. Characterization of the modified materials

Thermogravimetric analyses (TGA) were recorded on a Mettler Toledo TGA-DSC 3+. The measurements were performed in a continuous flow of oxygen and the samples were heated from 30 to 600 °C with a heating rate of 10 °C/min. The modification degree (Mod. deg.) in number of organic groups per nm² (groups/nm²) can be calculated from the weight loss of the burned carbon group by using the following formula:

$$mod.dg.\left(\frac{groups}{nm^2}\right) = \frac{wt\%(R) * N_A}{MM(R) * S_{BET}}$$

In which *wt%(R)* is the weight loss percentage in g/100g of sample of removed organic group as measured in TGA, *MM(R)* is the molar mass of the carbon group, S_{BET} is the surface area of the unmodified TiO_2 and N_A is Avogadro's constant. The experimental error is estimated to 0.1 groups/nm² based on five repeated measurements of a sample.

The diffuse reflectance infrared Fourier transform (DRIFT) measurements were performed on a Nicolet 6700 Fourier Transform IR spectrometer, equipped with an electromagnetic source in the mid infrared region (4000 – 400 cm^{-1}) and a DTGS detector. A resolution of 4 cm^{-1} was used and for each spectrum 100 scans were accumulated. The sample holder contained a 2 wt% diluted sample in KBr and was measured after 30 min at 150 °C under vacuum to remove the molecular adsorbed water. Since spectra were taken under vacuum, no subtraction of water or CO_2 signals was necessary.

X-ray photoelectron spectra (XPS) were recorded using a PHI5600 photoelectron spectrometer (Physical Electronics) with an Al Kα monochromatic X-ray source (1486.71 eV

photon energy). The vacuum in the analysis chamber was 1×10^{-8} Torr. A survey with a high-sensitivity was recorded with a pass energy of 187.85eV from a spot diameter of 0.8 mm. High-resolution scans of the main elements were recorded with a pass energy of 23.5 eV and an energy step size of 0.1 eV. XPS data are analyzed using PHI MultiPak software (v9.5). The energy scale of the XPS images was calibrated relative to the binding energy of the C1s peak (C−C/C−H) and set to 284.7 eV. The powders were applied on Indium foil (pressed in this soft metal)

X-band continuous wave (CW) EPR measurements were performed on a Bruker ESP300E spectrometer with a microwave frequency of ~9.45 GHz, equipped with a gas-flow cryogenic system (Oxford Instruments), allowing for operation from room temperature down to 2.5 K. The spectra were recorded with a modulation amplitude of 0.5 mT at a modulation frequency of 100 kHz, and microwave power of 25 mW at room temperature or 1 mW at 25 K.

3. Results and Discussion

3.1. Standard modification on P25

P25 was modified using organic groups with different chain lengths following the basic modification protocol described in 2.3. The modification degrees are shown in Table 2. It is clear that, with an increase in chain length, the modification degree decreases. This is similar to the trend observed by Yamamoto *et al.* for the modification of MCM-41[54] and by S. Rezaei Hosseinabadi *et al.* for the modification of ceramic membranes[26] with Grignard reactants, where a decrease in modification degree was observed with increasing size of the Grignard reactant used. It should be noted that MCM-41 and the membranes modified by S. Rezaei Hosseinabadi *et al.* were porous, while the P25 used here is not, indicating that the observed differences were more likely to be inherent to the modification itself rather than diffusion inside nanometer sized pores, although effects from both cannot be excluded.

Some differences can be seen when comparing the IR spectra of unmodified P25 samples before and after vacuum treatment and the modified P25 samples (Figure 1 showing the 3900 cm^{-1} - 2600 cm^{-1} region (A) and the 1900 cm^{-1} – 900 cm^{-1} region (B), Full spectra can be found in Appendix A Figure A.3). Firstly, it is clear that the vacuum treatment has caused changes to the P25 support. New signals between 1100 cm^{-1} and 1750 cm^{-1} are visible. It has been reported that a vacuum treatment can result in a disorganized outer layer on P25,[55] but it is uncertain if this outer layer is responsible for the appearance of these new signals.

Organic group	Mod deg. (groups/nm²)*
Ethyl	1.2
Propyl	0.6
Octyl	0.4

*Table 2: Modification degree of P25 modified with different Grignard reactants. *calculated from TGA weight loss between 250 °C and 500 °C(experimental error 0.1groups/nm²).*

Moreover, when a blank sample was prepared, using all process steps including washing, except for the addition of the Grignard reactant, these signals are also altered again, and changes are also observed in the OH-region (2900 cm^{-1} - 3800 cm^{-1}). Therefore, these spectral changes are likely due to the influence of the solvent and the washing steps. After modification, peaks at 2960 cm^{-1}, 2875 cm^{-1}, 2930 cm^{-1} and 2857 cm^{-1} are visible due to the presence of CH_3 and CH_2 stretching vibrations of the alkyl group grafted on the surface (Figure A.3).[44] P25 also shows some, less intense, signals in this region, most likely due to organic contaminants in the commercial powder. These contaminants are also observed in XPS (Figure 2). In the region between 1100 cm^{-1} and 1700 cm^{-1} changes occurred as well (Figure 1B). While the signals at 1550 cm^{-1} and 1360 cm^{-1} might be due to the vacuum treatment, a new, relative intense signal at 1435 cm^{-1} can be seen. This signal may be attributed to the C-C deformation vibration.[56] A signal at 1615 cm^{-1} is visible as well, but as it is in the region where also residual molecular adsorbed water can contribute, it is difficult to unambiguously assign this signal.[57–59] It is possible that these two signals

(1615 cm^{-1} and 1435 cm^{-1}) are caused by carboxylate ions on the surface[60], originating from the acetic acid washing. This is however less likely since the signal at 1435 cm^{-1} is not present in the blank sample that had the same acetic acid washing. Still, some binding energies due to C-O and C=O where observed in the XPS measurement of P25 modified with ethylmagnesium bromide (Figure 2, C1s) but since similar signals are also observed for unmodified P25 and the sample after the first washing step (and before the acetic acid wash) it is uncertain if these signals are caused due to acetic acid or contaminants that adsorb on the surface after exposure to ambient air.

It is clear that some signals present in the vacuum-treated sample have also disappeared. However, they also disappeared in the blank sample so these differences could be due to the reaction and washing conditions. The region between 3500 cm^{-1} to 3730 cm^{-1} also shows changes (Figure 1A). In this region the vibrations of the surface hydroxyl groups of titania and molecular adsorbed water can be found. After modification, the relative intensities of the signals in this region have increased (most clearly visible in Figure 1A, e) and the maximum has shifted towards higher wavenumbers (3670 cm^{-1}) compared to unmodified P25 after vacuum treatment (3660 cm^{-1}) and the blank, even though the original signals are still visible as a shoulder. It is important to note that the relative intensity of this new signal is not correlated to the modification degree. It is, however, not clear what the underlying reason is. This signal at 3670 cm^{-1} is due to hydroxyl groups of the anatase crystal phase.[61] Another new signal (shoulder at 3720 cm^{-1}) has also appeared which can most likely be attributed to isolated hydroxyl groups.[62] Based on these changes, it can be concluded that during the modification new hydroxyl groups seem to have formed or hydroxyl groups, that were present, have changed in their direct coordination and/or bond strength, due to changes induced by the modification. Different mechanisms can result in the formation of new -OH groups. One possibility is that the Grignard reactant breaks Ti-O-Ti bonds, similar as the

observed Si-O-Si breaking during the modification of silica.[31,32] Another possibility is that new hydroxyl groups are formed because of a reaction of Ti(III) (see later) and water or acid during the washing. Alternatively, the presence of Ti(III) sites might result in differences in the bond strength of the hydroxyl group or the presence of the alkyl group might break vicinal surface OH groups, resulting in isolated sites. Since these changes are not present in the blank sample (Figure 1A, spectrum c) it is certain that these changes are not due to merely the solvent and conditions of the synthesis nor the washing step.

To be sure that the changes in the OH region of the FTIR spectra are only due to the formation of new hydroxyl groups on the titania surface originating from the reaction with the Grignard reactant and not due to an unwashed contaminant from the modification, a sample modified with ethylmagnesium bromide, was studied by XPS. After the first washing step (with THF under inert atmosphere), the presence of magnesium was detected (Figure 3). To determine the state of the magnesium by looking directly at the binding energies of the Mg signals is less straightforward, since differences in binding energy are small (~1eV)[63,64]. Therefore, besides the binding energy, the auger parameter can also be used.[63]

$$\alpha = KE(Mg1s) - KE(MgKLL)$$

$$KE = kinetic\ energy = \ h\nu - BE - \phi$$

BE = binding energy

Since the excitation energy (Al Kα 1486.6 eV) and the work function of both MgKLL and Mg1s are the same, we can directly use the binding energies (determined from the survey in Figure 2A) to calculate the auger parameter. In literature a auger parameter of 998.6 eV is found for MgO.[63] The value found here, 998.3 eV, is within the energy resolution of the instrument. We can therefore conclude that a MgO contamination is present on the surface.

$$\alpha = BE(Mg1s) - BE(MgKLL)$$

$$\alpha = 1303.9\ eV - 305.6\ eV$$

$$\alpha = 998.3\ \text{eV}$$

The same sample has also been measured after full washing (Figure 2, red curve). No Mg signal was detected (Figure 2). This indicates that the washing used is rigorous enough and that the changes observed in the OH region can only be due to the formation of new surface hydroxyl groups and not by unwashed magnesium oxide residues.

An important observation is that during the modification, a color change of the P25 takes place when the Grignard reactant is added to the titania. This color change has been reported before[44] and has been linked to the reduction of titania, although no experimental proof was provided. Here, the presence of Ti(III) was confirmed by EPR.

Figure 4 shows the cw X-band EPR spectra of octyl and ethyl-modified P25 recorded at 25 K after full washing and exposure to ambient atmosphere. In both spectra, a signal centered at around 370 mT (g ~ 1.95) is observed. Similar spectra have been reported for other Ti(III) containing materials and has been attributed to isolated Ti(III) sites.[65] This signal is more intense in the case of ethyl modified P25 compared to octyl modified P25, which appears to correlate with the higher degree of modification of the shorter alkyl chained reactant. On the other hand, the room temperature EPR spectrum of ethyl modified P25 is relatively silent, while a very weak broad signal between 200 to 400 mT is visible in the spectrum of octyl modified P25, which is tentatively assigned to antiferromagnetically coupled Ti(III) centers within the bulk of the material (Figure 4). Further in-depth investigation of this reduction mechanism and how it is related to the change in color is not within the scope of this publication and will be the focus of a separate paper. For the sample modified with octylmagnesium chloride we note that some Cu(II) contamination is present, most likely caused by using copper-contaminated glassware.

All further experiments have been performed with octylmagnesium chloride as the Grignard reactant since the octyl group is easier to characterize than propyl or ethyl. The P25 modified with octylmagnesium chloride at room temperature will be referred to as the standard material, employed for comparison of the other samples in order to illustrate the differences induced by the changes in the synthesis conditions and/or TiO_2 supports.

3.2. Determining the influence of the concentration of the Grignard reactant

The modification degree for the reference sample is quite low, especially compared to other modification methods. As seen in 3.1, Grignard modification results in 0.4groups/nm² modification while organophosphonic acid modification can have a modification degree up to ~3 groups/nm² as reported in literature.[20,21] Therefore, it is interesting to evaluate if higher concentrations of the Grignard reactant might increase the modification degree, as is the case of silica.[34] However, higher concentrations could also induce more possible side reactions/products. For these experiments, four different amounts of Grignard reactant (2, 3, 4 and 6 mmol) were used. The first noticeable difference was observed during the first washing step: the time the THF needed to filtrate through the filter was two to three times longer for the samples modified with 4 and 6 mmol of Grignard reactant. To test if this observation was reproducible, the experiments were performed three times, each time with similar differences in filtration time.

The TGA and DTG are shown in Figure 5 (a close-up of 2 mmol, 3 mmol and 6 mmol after extra wash can be found in section 5.1). When looking at the weight losses from the TGA measurement, a sudden increase in weight loss can be seen when 4 and 6 mmol of Grignard is used. These TGA results suggest a positive influence of the concentration on the modification degree, but when the materials are studied by IR measurements (Figure 6 (A: region 3900 cm^{-1} to 2600 cm^{-1}, B: region 1900 cm^{-1} to 900 cm^{-1}) and Figure A.4), a different conclusion can be made.

The 4 mmol and 6 mmol samples that displayed a sharp TGA signal, show additional IR signals for magnesium oxyhydroxides[66]. At 3695 cm^{-1} a very sharp and intense signal from the Mg-OH stretch vibration can be seen, while other typical signals for MgO and $Mg(OH)_2$ are visible at 1420 cm^{-1} and 1540 cm^{-1} .[66] The sample modified with 2 mmol octylmagnesium chloride does not show the sharp signal at 3695 cm^{-1} but the sample modified with 3 mmol does have a small signal around this position. This is shown in a close-up of the OH region in section 5.1.

Amount octylmagnesium chloride added	2 mmol	3 mmol	4 mmol	6 mmol	6 mmol extra wash
wt%*	0.4	0.5	1.5	1.6	0.6
Mod. deg. (groups/nm^2)*	0.4	0.5	n.a.	n.a.	0.6

*Table 3: weight percentage loss (wt%) and modification degree of P25 modified samples with different amounts of octylmagnesium chloride *calculated from TGA weight loss between 250 °C and 500 °C(experimental error 0.1groups/nm^2).*

Both the 2 mmol and 3 mmol sample possess a shoulder around 1420 cm^{-1} (Figure 6B). However, as it is also present in the unmodified P25 (Figure 6a) it cannot be unambiguously assigned. The sample modified with 6 mmol was further examined with XPS (Figure 7 and Figure 8). Mg was clearly detected in combination with a shoulder in the O1s peak. When compared to the signal of the MgO species, as reported in Figure 3, it is clear that the signal detected for the sample modified with 6 mmol of octylmagnesium chloride shows additional signals at higher binding energies (Figure 7).

This indicates the presence of $Mg(OH)_2$ although MgO will still be present as well. We therefore conclude that the signals in the IR spectra are caused by magnesium oxyhydroxide species on the surface. For the C1s signal (Figure 8), a new peak around 290 eV can be seen, indicative for the presence of carbonate species. Most likely this is remaining acetic acid

from the washing. However, no significant carbonate signals can be seen in the IR spectrum (Figure A.4 spectrum e).

To evaluate if the magnesium oxyhydroxides could be removed, the sample modified with 6 mmol of octylmagnesium chloride underwent an extra washing by stirring the sample in acetic acid (0.1 M) overnight at 60 °C. Afterwards, the sample was filtered and dried in ambient air. To be sure that all acetic acid would be removed, the sample was further washed with water (90 mL) at 90 °C. The TGA results are shown in Figure 5 and Table 3 denoted as "6 mmol extra wash". After washing, the strong weight loss observed before the washing has disappeared and the wt% lost becomes similar but slightly higher (0.6 groups/nm²) compared to the samples modified with 2 or 3 mmol octylmagnesium chloride, 0.4 and 0.5 groups/nm² respectively. These differences in modification degree are close to the experimental error of the measurement but reproducible. In the XPS, no magnesium can be measured (only noise) and the shoulder in the O1s signal has disappeared (Figure 8). Similarly, in the infrared spectrum, the sharp signal at 3695 cm^{-1} has disappeared, coinciding with disappearance of the broad signals at 1420 cm^{-1} and 1540 cm^{-1}, confirming the XPS results. The IR spectrum is now similar to the sample modified with 2 mmol octyl magnesium chloride, showing similar signals as discussed for Figure 1. Nevertheless, some differences remain. The 6 mmol washed sample shows a clearer signal at 3720 cm^{-1} compared to the 2 mmol sample (Figure 6A dashed line), indicating that more isolate hydroxyl groups have been formed. Thus the increased amount of Grignard reactant during the modification seems to promote the formation of more isolated hydroxyl groups on the surface, that can originate from different mechanisms as described in 3.1.

Based on these results we can conclude that using a higher amount of Grignard reactant results in only a small increase in the modification degree of 0.2 groups/nm² or 0.02 mmol/g P25. The downside is that more washing is required to remove all side products from the

surface. This is in contrast with modifying silica materials. Bein *et al.*[34] reported that when modifying silica materials, increasing the amount of Grignard reactant (*n*-butylmagnesium chloride) from 0.125 M to 0.2 M (compared to 0.067 M to 0.2 M in this study) resulted in an increase of around 0.2 mmol of *n*-butyl groups/g MCM-41. This is 10 times higher than the increase observed here. Similar to the modification on silica, some evidence indicates that higher concentrations of Grignard reactant lead to more metal-oxygen bond breaking as an increase in isolated hydroxide species is apparent, but an increase in the support reduction might also cause this.

3.3. Evaluating the influence of reaction time

In the present study 72 h was the standard reaction time. To study the impact of reaction time, the reaction was stopped after 4, 24 and 48 h. All other parameters were kept constant: octylmagnesium chloride (2 mmol), and the reaction was performed at RT under argon atmosphere.

Figure 9 shows the TGA and the first derivative of the TGA measurement for all samples and the unmodified P25 as a reference. All modified samples show a clear but broad weight loss between 300 and 500 °C. No significant differences can be seen, only the sample reacted for 72 h shows a slightly higher weight loss around 450 °C. The modification degree for all samples are around 0.4 groups/nm² and within the error of measurement of the equipment (0.1 groups/nm²) as can be seen in Table 4. A longer reaction time does not seem to result in an increased modification degree. The results are also different compared to the Grignard modification on silica. Bein *et al.*[34] reported an increase from 1.5 mmol g^{-1} to 4.0 mmol g^{-1} on MCM-41 within the first 24 h. Longer reaction times were not reported so it remains unclear if a further increase in the modification degree would occur upon longer reaction times. The remaining amount of Grignard reactant after modification has been determined by

titration with I_2.[53] After 4h 20% of the Grignard reactant is still remaining. After 24h, no Grignard reactant could be detected.

Reaction time	4 h	24 h	48 h	72 h
Mod. Deg. (groups/nm²)*	0.4	0.3	0.3	0.4
Grignard remaining**	20	0	0	0

*Table 4: Modification degree and percentage of Grignard remaining after different reaction times.*calculated from TGA weight loss between 250 °C and 500°(experimental error 0.1groups/nm²). ** determined by titration with I_2*

To confirm this result, an aliquot of the reaction mixture was quenched with D_2O after 24 h, as described in 2.4, and no deuterated octane could be observed in the GC-MS. To verify this trend of a strong decrease within the first 4 h, a similar titration experiment on P25 samples modified with propylmagnesium chloride was performed. The results, shown in Figure 10, indicate a similar trend for both the propyl and octyl Grignard, although the percentage of the remaining octylmagnesium chloride decreases faster. The fact that the strongest decrease happens within the first 4 h supports the observations from TGA representing a constant value of the modification degree. Hence, the maximum surface modification degree is reached after less than 4h under these conditions.

3.4. Elucidating the influence of the reaction temperature

To study the impact of the temperature, modifications at -78 °C, room temperature and 65 °C were performed. Reaction times of 4 h and 24 h were used to determine if the time to reach maximum surface modification would be influenced by the reaction temperature. The modifications were performed using a Schlenk line instead of in a glove box, to allow easy heating or cooling of the reaction mixtures.

When working at different temperatures, several changes can be observed. The first difference is the color change. During modification at RT, the color change takes more than 10 min and the mixture turns grey. However, when working at 65 °C the change in color takes less than 5 min and the mixture becomes dark grey-blue. Whereas, at -78 °C the color

change takes more than 30 min and turns only light grey. This indicates that the temperature has an impact on the kinetics of the reduction of the titania, expected to be responsible for the black coloration.[67–69] After modification and washing, the difference in color persists for the sample modified at 65 °C. This sample remains colored (blue), while the samples modified at room temperature and -78 °C have become white after being exposed to the ambient atmosphere. The difference can be seen in Figure A.5. (Appendix A). As mentioned before, the blue color can be linked to the presence of Ti(III) centers. In Figure 11 the EPR spectra are reported for P25 modified at 65 °C and at RT after full washing. It is clear that the intensity of the Ti(III) signal recorded at 25 K has increased drastically when modifying at 65 °C compared to RT. The increase in temperature allows for a more extensive reduction of the titania support.

Even though the color changes of the samples are significantly different, the weight losses measured with TGA are comparable (TGA and DTG profiles in Figure12). As can be seen in Table 5, the modification degree is independent of the temperature and modification time (similar as discussed previously). Only the sample modified at 65 °C for 4 h shows a slightly lower modification degree but this difference is within the experimental error. Hence, it seems that the temperature influences the electron transfer during the reaction, causing the reduction of the sample (and thus the change in color), but has no significant impact on the formation of the organic layer. It indicates that the surface modification is a fast process with no observable impact of temperature when the latter is between -78 °C and 65 °C (we don't know how the kinetics could be influenced at lower temperatures). The reduction process kinetics is on the other hand clearly affected by temperature variations between -78 and 65 °C. It tends to indicate that both processes are not directly linked, the electron transfer having no significant impact on the functionalization process.

Again, this is different from the observations by Bein et al.[34] For the modification of silica, the number of organic groups on the surface increased from 0.7 mmol/g to 3 mmol/g when modifying MCM-41 at 68 °C (reflux temperature of THF) for 4 h.

Reaction time	temperature	Mod. Deg. (groups/nm²)*
4h	-78 °C	0.4
	RT	0.4
	65 °C	0.3
24h	-78 °C	0.4
	RT	0.4
	65 °C	0.4

*Table 5: Modification degree of P25 modified with octylmagnesium chloride at different temperatures and times. *calculated from TGA weight loss between 250 °C and 500 °C (experimental error 0.1groups/nm²).*

In the IR spectra of the modified P25 (Figure 13B and Figure A.6), small changes in the 1100 cm^{-1} to 1700 cm^{-1} region can be seen between the different modified samples. The most significant difference is the change in the OH region (3500 cm^{-1} -3750 cm^{-1}) for the sample modified at 65 °C for 24 h (Figure 13A, spectrum f). This sample exhibits a more intense signal at 3720 cm^{-1} (higher relative contribution) attributed to isolated hydroxyl groups compared to the other samples. Hence, the increased temperature seems to influence the formation of this new OH-signal, that can originate from different mechanisms as described above. As the modification degree does not change, this new OH signal seems to be correlated to the breaking of Ti-O-Ti bonds or the Ti(III) formation (which can be seen from the darker color for the samples at 65 °C).

Hence, the mechanism for the new OH-signal and the modification reaction itself, seem to be independent from each other. A similar conclusion can be made when looking at the OH region for the sample modified at -78 °C for 4h (Figure 13A spectrum d). Almost no change

in the OH region compared to the unmodified P25 (Figure 13A spectrum a) is present, but the modification degree is similar to the other samples.

This is different for the modification of silica[31,32,34] where a clear correlation between the temperature and modification degree has been observed. Moreover, a higher number of grafted groups to the surface was always accompanied by an increase in the Si-O-Si breaking. It is important to mention that an electron transfer process has not been reported for the Grignard surface modification of silica. This could be the reason why differences are observed between the two support materials.

3.5. Does the TiO_2 support material properties play a role?

In all previous experiments non-porous P25 has been used as the support material. Although for silicon supports, the porosity has been reported to play an important role in the modification mechanism,[38–42] the impact of physico-chemical properties of the support material (e.g. phase composition) has not been reported yet.. Therefore, to test the impact of the physico-chemical support properties on the modification and the amount of groups grafted, various titania supports have been modified.

The experimental set consisted of five types of titania samples. The commercially available P25, CristalActiv PC500 after calcination at 470 °C and three lab synthesized titania. All information on the supports can be found in 2.1. All samples have been modified with octylmagnesium chloride (2 mmol) for 24 h at room temperature under argon atmosphere. Clear differences can already be seen during the modification. Firstly, the color change of the samples is not always the same. P25 becomes blueish grey, PC500 only light grey, TiO_2 HCl becomes gray, while TiO_2 H_2SO_4-1 and sTiO_2 turn dark grey, almost black in color (Figure A.7, Appendix A).

Besides the color itself, also the rate of these color changes differs between the samples. The commercial samples (P25 and PC500) took 10 to 15 min to get their darkest color, while the other samples changed within a few minutes.

When comparing the modification degree of these samples, the influence of the titania support on the modification can clearly be seen (Table 6). Depending on the type of titania support material, a modification degree per nm² that is up to 2 times higher than on the commercial P25 can be reached, using the same reaction conditions. Moreover, besides the modification degree, also a shift in the temperature range of the weight loss in TGA can be seen in the DTG, dependent on the type of support (Figure 14). For P25 the weight loss occurs between 250 °C and 500 °C, for PC500 this is between 200 °C and 500 °C, TiO_2 HCl has a weight loss between 250 °C and 450 °C, TiO_2 H_2SO_4-1M between 150 °C and 400 °C and sTiO_2 between 200 °C and 400 °C. Similar shifts have been reported before for the modification of TiO_2 with organophosphonic acids in toluene[21]. With an increase in the number of grafted organophosphonic groups onto the surface, the ordering in the organic layer increased and shifted the weight loss to lower values. A similar phenomenon could be the case here, where higher modification degrees could lead to an increase in the order of the organic layers on the different supports. Nevertheless, other phenomena such as the impact of Ti(III) formation, which is clearly different in the different supports, as indicated by the differences in color, or a difference in type of Ti site on which the functional group has bonded as induced by the difference in crystal and amorphous content, cannot be excluded.

	Color	Mod. Deg. (gr/nm^2)*	Amorphous content (%)**	Anatase content (%)**	Other crystal phase (%)**
P25	Blueish grey	0.4	4	83	Rutile (13)
PC500	Light grey	0.5	8	91	/
TiO_2 HCl	Grey	0.7	15	85	/
TiO_2 H_2SO_4 -1	Dark grey	0.8	28	67	Rutile (5)
sTiO_2	Dark grey	0.9	31	59	Brookite (9)

*Table 6: Color, modification degree and the crystal and amorphous content of different titania supports.*determined by TGA, experimental error 0.1 groups/nm², **determined by EELS (experimental error 2%)*

By comparing the different samples, information can be gained on which properties of the titania might influence the modification. Noticeably the samples that had the darkest color change have the highest modification degree, the samples with a lighter color have less organic groups. It should, however, be noted that this is not necessarily correlated as observed when modifying at different temperatures. Another possible factor that might play a role can be the crystal phases and crystal content in the supports. Using Electron Energy Loss Spectroscopy (EELS) the crystal phases were qualified and quantified and the amount of amorphous phase determined in the different supports (Figure A.8, Appendix A). An overview is given in Table 6. All samples are composed, for a substantial percentage, of anatase and P25, TiO_2 H_2SO_4-1 and the sTiO_2 also feature a second crystal phase next to a non-negligible amorphous phase. P25 has 13% rutile, TiO_2 H_2SO_4-1 has 5% rutile, while the sTiO_2 has 9% brookite. When comparing the material composition with the modification degree no correlation between the anatase content and the modification degree seems to exists. Brookite could have a positive influence in the case of the TiO_2 flakes but it seems unlikely that only this minor amount of brookite results in such a high modification degree compared to the other samples. More likely is that, not the crystal part of the titania, but the amorphous titania content in the samples is the key. P25 and PC500 are very crystalline

materials with ± 4% and ± 8% of amorphous phase, respectively. The other porous samples have much higher contents of amorphous titania. It is clear that these samples also exhibit much higher modification degrees. Even though the correlation is not linear, it is apparent that it follows the same upward trend with the amorphous fraction. The amorphous phase might be more susceptible to an attack of the Grignard reactant due to its high concentration in defect sites,[70] resulting in a higher modification degree. Still, this is only a hypothesis since EELS measures the different phase of the bulk material and not only those present on the surface. More research is needed. Furthermore, it is possible that not only the surface reaction is important, but that a transport of the reducing electrons towards the bulk is needed as well to achieve higher modification degrees.

Another factor could be the presence of (surface) anions. All samples have been synthesized with the aid of different additives, which can remain to some extent in the structure. P25 and TiO_2 HCl have (a low amount) of chloride ions in their structure. Chloride ions only have a weak interaction with the TiO_2 surface.[71] PC500 and TiO_2 H_2SO_4-1 have sulfate ions in their structure, which interacts strongly with the titania.[72,73] Similarly, nitrate ions are present in sTiO_2 that also have a strong interaction. Since all these anions interact differently with the titania surface, definite conclusions cannot be made based on this base set of five titania. Furthermore, it is not straightforward to change the ion content in titania without changing the amorphous and crystal content to validate this hypothesis. Moreover, as the correlation with the amorphous content is not linear, both the amorphous content as well as other contributing factors such as, but not limited to, ion type and content and distribution on surface vs. bulk and the distribution of crystal or amorphous phase in the bulk vs. the surface could be at play.

To validate/exclude these hypotheses, two additional supports have been modified. These titania (TiO_2 H_2SO_4-0.1 and TiO_2 H_2SO_4-0.01) were synthesized using the same procedure

as TiO_2 H_2SO_4-1 but during the synthesis a lower concentration of sulfuric acid (0.1 or 0.01 M) has been used. A decrease in the amount of SO_4^{2-} anions in the resulting titania has been confirmed by SEM-EDX. At the same time, the amorphous content of these materials also changes inversely proportional. The atomic percentages, amorphous content (EELS) and modification degrees (deduced from TGA, Figure 14) are shown in Table 7. The results clearly show that the modification degree increases with increasing amorphous content, while the change in modification degree is not correlated or inversely correlated to the ion content. Although these results support the hypothesis of a correlation between amorphous content and enhanced modification degrees, it does not allow to exclude a possible coinciding (negative) role of residual ions in the material. It remains therefore unclear whether the presence of anions on the surface has a significant impact on the modification degree.

Support	TiO_2 H_2SO_4-1	TiO_2 H_2SO_4-0.1	TiO_2 H_2SO_4-0.01
Sulfur content (%)	3.09	0.41	n.d.*
Amorphous content (%)	28	34	46
Mod. Deg. (groups/nm²)	0.8	1.0	1.2

*Table 7:Sulfur content, amorphous content and modification degree of different TiO_2 H_2SO_4 supports. *n.d.= not detected.*

3.6. Does the TiO_2 support influence the impact of the other reaction conditions?

While it is clear that the support properties impact the number of organic groups on the surface, it is uncertain if they also influence how the other reaction conditions impact the modification. Therefore, the same reaction parameters that were tested for P25 were also investigated for the modification on sTiO_2 and are discussed briefly below.

3.6.1. Understanding the impact of the chain length

Organic group	Modification degree (groups/nm²)
Ethyl	1.5
Propyl	1.0
Octyl	0.85

Table 8: modification degrees of sTiO2 modified with different Grignard reagents calculated from the TGA weight loss between 200 °C and 400 °C.

Similar as for P25 (Table 2), the modification degree decreases as the chain length increases (Table 8), in a non-linear way. Different with the modification on P25 is that after modification with ethylmagnesium bromide, the fully washed sample did not retain its color. This hints to a support effect also in the reduction (Ti(III) formation) mechanism. This can also be seen in Figure 15 where bulk reduction is observed in the RT spectra, while no isolated Ti(III) centers or only a small amount are observed in the 25 K spectra.

3.6.2. Determining the influence of the concentration of the Grignard reactant

The TGA and DTG of $sTiO_2$ modified with different amounts of octylmagneisum chloride can be seen in Figure 16. To remove all magnesium contaminants, the samples modified with 4 mmol and 6 mmol of octylmagnesium chloride underwent an extra washing as described in 3.2. The successful washing is confirmed by the absence of Mg signals in the infrared spectra (Figure 17 and Figure A.9). From Table 9 it is clear that no significant changes (within 0.1 gr/nm²) in the number of grafted groups has occurred. This is different when compared to P25 where a small increase was observed. The reason for this difference is unclear at this time. Just as was described for P25, also for $sTiO_2$ we see an increase in the relative intensity for the isolated hydroxyl groups (3720 cm^{-1}) on the TiO_2 surface when using 6 mmol of Grignard reactant (Figure 17A). Besides an increase of the signal, also a broadening of the peak at 3720 cm^{-1} takes place for all samples when compared to 2 mmol. Reasons for these changes in the hydroxyl regions have been given in section 3.1. A signal at 1540 cm^{-1} also increases in intensity when the concentration increases (Figure 17B).

Amount octylmagnesium chloride added	2 mmol	3 mmol	4 mmol extra wash	6 mmol extra wash
wt%	1.8	1.9	1.9	1.8
Mod. deg (groups/nm²)	0.9	0.9	0.9	0.9

Table 9: Calculated wt% and modification degree of $sTiO_2$ modified samples with different amounts of octylmagnesium chloride calculated from the TGA weight loss between 200 °C and 400 °C

3.6.3. Evaluating the influence of reaction time

When looking at the number of grafted organic groups on the surface, as shown in Table 10, no significant impact of the reaction time can be seen. The small variations are all with the 0.1 gr/nm² error of the equipment. All DTG profiles (Figure 18) are similar for all modified samples. Using the titration method the remaining amount of Grignard reactant was determined. No active Grignard reactant was present even after 4 h.

Reaction time	Reaction time	4 h	24 h	48 h	72 h
Mod. Deg. (groups/nm²)*	Mod. Deg. (groups/nm²)	0.8	0.9	0.9	0.8
Grignard remaining**	Remaining Gr (%)	0	0	0	0

*Table 10: Modification degree and percentage of Grignard remaining after different reaction times for the modification of $sTiO_2$.*calculated from TGA weight loss between 250 °C and 500°(experimental error 0.1groups/nm²). ** determined by titration with I_2*

3.6.4. Elucidating the influence of the reaction temperature

As we reported for P25, differences in the color changes for $sTiO_2$ modification have been observed as well. At 65 °C the color changes faster (within 30 s) and the mixture becomes darker compared to the modification at RT. At -78 °C the change is very slow (taking longer than 15 min) and only a light grey color is reached. After modification, all samples return to an off-white color. This is different compared to P25 where the sample modified at 65 °C remained blue. For P25 a strong increase in isolated Ti(III) was found using EPR (Figure 11). For $sTiO_2$ no strong increase in isolated sites is seen after full washing (Figure 19), indicating that the support clearly influences the reduction process. Also no significant change can be seen for the bulk reduction after full washing.

Reaction time	temperature	Mod. Deg. (groups/nm²)
4 h	-78 °C	0.8
	RT	0.8
	65 °C	0.8
24 h	-78 °C	0.8
	RT	0.9
	65 °C	0.9

Table 11: Modification degrees calculated from the TGA weight loss between 200 °C and 400 °C of $sTiO_2$ modified with octylmagnesium chloride at different temperatures and times.

For the samples modified at RT and 65 °C for 24h an increase in the weight loss between 200 °C and 350 °C can be seen (Figure 20), coinciding with a decrease in weight loss between 150 °C and 250 °C. This observation differs from what was observed for P25. The underlying reason is yet unclear. While these samples also show slightly higher modification degrees compared to the others (Table 11), these differences are not significant and within experimental error. Some differences can also be seen in the infrared (Figure 21 and Figure A.10). For the samples modified for 24 h significant differences can be seen in the hydroxyl region (Figure 21A), the samples modified for 4 h show less differences when comparing the different temperatures. The sample modified at 65 °C for 24 h also shows an increased signal intensity at 1550 cm^{-1}. The reason is unclear at this time. Both samples modified at -78 °C the signals below 1700 cm^{-1} are less pronounced compared to the samples modified at higher temperatures (Figure 21B).

4. Conclusion

In this publication, the impact of different reaction conditions on the Grignard surface modification of titania is described and compared to previously reported results on the modification of ordered mesoporous silica. During the modification, new signals of isolated hydroxyl groups appear in the infrared analysis, showing important changes of the titania

surface. When using Grignard reactants with increasing chain lengths, the modification degree decreases and less reduction of the support takes place (visible as Ti(III) in EPR). Higher Grignard concentrations result in the presence of magnesium oxyhydroxides requiring a more extensive washing process to remove them. Furthermore, more isolated hydroxyl groups seem to have been formed, without significantly increasing the amount of organic groups onto the surface. Different reaction times (> 4 h) show no significant impact on the modification degree. The reaction temperature appears to influence the reduction of the titania support and the formation of isolated OH-groups, but has no impact on the number of grafted organic groups, indicating that the reduction of the titania is not the rate-determining step in the modification and that it is, together with the formation of the isolated OH groups, a separate processes from the grafting of the organic groups. Interestingly, the most significant impact on the modification degree, is due to the titania support properties itself. In contrast to the temperature impact, in this case there seems to be both a correlation with the intensity of the color change and the modification degree, but no definitive conclusion could be made. And while it is not necessarily the only determining factor, it is clear that the amount of amorphous phase has a significant impact on the modification degree. The support properties only seem to change the modification degree but not the impact of the other reaction parameters on the modification degree. A clear impact of the support on the type of reduction is seen as well. These observations hint to a complex interplay of interactions and reactions during the Grignard modification. Extra studies to fully elucidate the underlying mechanisms are in progress.

5. Supplementary data

5.1. Detailed DTG measurements and IR spectra for P25 modified with different amounts of octylmagnesium chloride

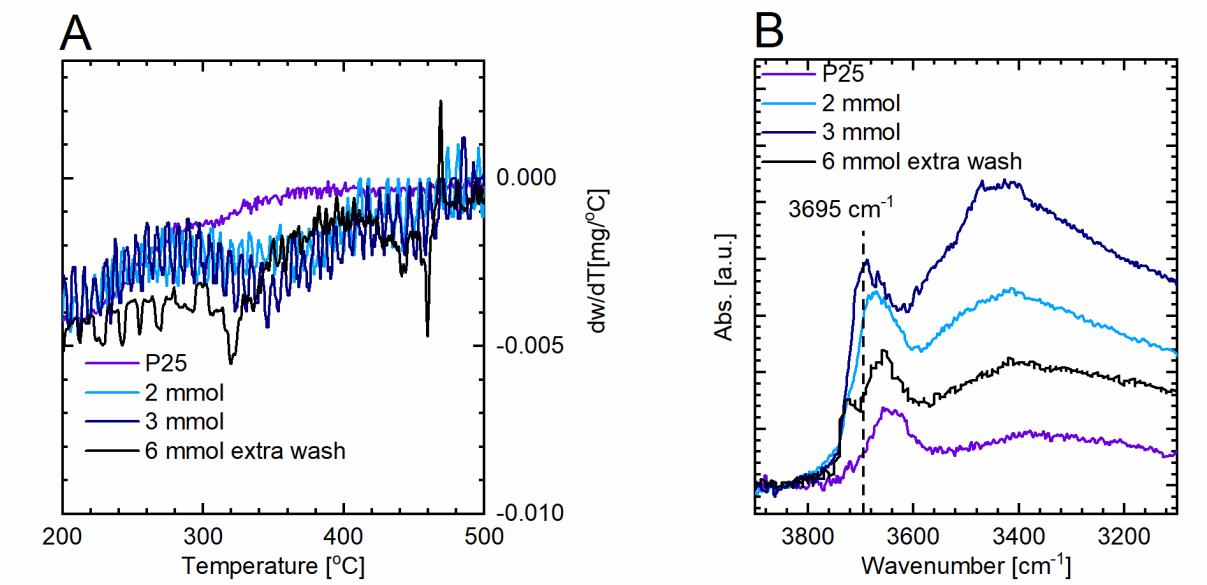

Detailed view of the DTG curve (A) and close-up of the infra-red OH region (B) for P25 modified with different amounts of octylmagnesium bromide.

Funding Sources

The FWO (Fonds Wetenschappelijk Onderzoek) is gratefully acknowledged for the VITO-FWO grant of fellow Jeroen G. Van Dijck (11W9416N) and the financial support granted in project GO12712N. The E.U. is acknowledged for H.Y. Vincent Ching's H2020-MSCA-IF (grant number 792946, iSPY). Dileep Krishnan and Johan Verbeeck acknowledge funding from GOA project “solarpaint” of the University of Antwerp.

Acknowledgment

The authors would like to thank Bharadwaj Mysore Ramesha for providing the amorphous powder standard used in EELS measurements. Thomas Kenis and Dr. Ing. Tom Breugelmans are thanked for the ICP-MS measurement to verify the absence of Mg after washing. Dr. Gert Nuyts is acknowledged for the SEM-EDX measurements.

References

[1] V. Meynen, H.L. Castricum, A. Buekenhoudt, Class II hybrid organic-inorganic membranes creating new versatility in separations, Curr. Org. Chem. 18 (2014) 2334–2350. doi:10.2174/1385272819666140806200931.

[2] S.R. Hosseinabadi, K. Wyns, A. Buekenhoudt, B. Van der Bruggen, D. Ormerod, Performance of Grignard functionalized ceramic nanofiltration membranes, Sep. Purif. Technol. 147 (2015) 320–328. doi:10.1016/j.seppur.2015.03.047.

[3] C.W. Hsu, L. Wang, W.F. Su, Effect of chemical structure of interface modifier of TiO_2 on photovoltaic properties of poly(3-hexylthiophene)/TiO_2 layered solar cells, J. Colloid Interface Sci. 329 (2009) 182–187. doi:10.1016/j.jcis.2008.10.008.

[4] N. Adden, L.J. Gamble, D.G. Castner, A. Hoffmann, G. Gross, H. Menzel, Phosphonic acid monolayers for binding of bioactive molecules to titanium surfaces., Langmuir. 22 (2006) 8197–204. doi:10.1021/la060754c.

[5] A. Mitrofanov, S. Brandès, F. Herbst, S. Rigolet, A. Bessmertnykh-Lemeune, I. Beletskaya, Immobilization of copper complexes with (1,10-phenanthrolinyl)phosphonates on titania supports for sustainable catalysis, J. Mater. Chem. A. 5 (2017) 12216–12235. doi:10.1039/c7ta01195d.

[6] S.P. Pujari, L. Scheres, A.T.M. Marcelis, H. Zuilhof, Covalent surface modification of oxide surfaces, Angew. Chemie - Int. Ed. 53 (2014) 6322–6356. doi:10.1002/anie.201306709.

[7] H. Deuel, J. Wartmann, K. Hutschneker, U. Schobinger, C. Güdel, Organische Derivate des Silikagels mit Si-O-C-Bindung I, Helv. Chim. Acta. 42 (1959) 1160–1165. doi:10.1002/hlca.19590420407.

[8] J.J. Pesek, S.A. Swedberg, Allyl-bonde stationary phase as possible intermediate in the

synthesis of novel high-performance liquid chromatographic phases, J. Chromatogr. A. 361 (1986) 83–92.

[9] T. Hara, S. Futagami, W. De Malsche, G. V. Baron, G. Desmet, Exploring the effect of mesopore size reduction on the column performance of silica-based open tubular capillary columns, J. Chromatogr. A. 1552 (2018) 87–91. doi:10.1016/j.chroma.2018.03.050.

[10] A.Y. Fadeev, T.J. McCarthy, Self-assembly is not the only reaction possible between alkyltrichlorosilanes and surfaces: monomolecular and oligomeric covalently attached layers of dichloro- and trichloroalkylsilanes on silicon, Langmuir. 16 (2000) 7268–7274. doi:10.1021/la000471z.

[11] K. Vrancken, P. Van Der Voort, K. Possemiers, E.F. Vansant, Surface and structural properties of silica gel in the modification with γ-aminopropyltriethoxysilane, J. Colloid Interface Sci. 174 (1995) 86–91. http://www.sciencedirect.com/science/article/pii/S0021979785713677 (accessed October 3, 2014).

[12] E. Vansant, P. Van Der Voort, K. Vrancken, Characterization and chemical modification of the silica surface, Elsevier Science, Amsterdam, 1995.

[13] K.. Vrancken, K. Possemiers, P. Van Der Voort, E.. Vansant, Surface modification of silica gels with aminoorganosilanes, Colloids Surfaces A Physicochem. Eng. Asp. 98 (1995) 235–241. doi:10.1016/0927-7757(95)03119-X.

[14] H.P. Boehm, Chemical Identification of Surface Groups, Adv. Catal. 16 (1966) 179–274. doi:10.1016/S0360-0564(08)60354-5.

[15] W. Gao, L. Dickinson, C. Grozinger, F.G. Morin, L. Reven, Self-Assembled Monolayers of Alkylphosphonic Acids on Metal Oxides, Langmuir. 12 (1996) 6429–6435. doi:10.1021/la9607621.

[16] R. Helmy, A.Y. Fadeev, Self-Assembled Monolayers Supported on TiO2 : Comparison of C18H37SiX3 (X = H , Cl , OCH3), C18H37Si(CH3)2Cl , and C18H37PO(OH)2, Langmuir. 18 (2002) 8924–8928.

[17] P.J. Hotchkiss, M. Malicki, A.J. Giordano, N.R. Armstrong, S.R. Marder, Characterization of phosphonic acid binding to zinc oxide, J. Mater. Chem. 21 (2011) 3107. doi:10.1039/c0jm02829k.

[18] P.H. Mutin, G. Guerrero, A. Vioux, Hybrid materials from organophosphorus coupling molecules, J. Mater. Chem. 15 (2005) 3761–3768. doi:10.1039/b505422b.

[19] J. Randon, P. Blanc, R. Paterson, Modification of ceramic membrane surfaces using phosphoric acid and alkyl phosphonic acids and its effects on ultrafiltration of BSA protein, J. Memb. Sci. 98 (1995) 119–129. http://www.sciencedirect.com/science/article/pii/037673889400183Y (accessed August 11, 2014).

[20] A. Roevens, J.G. Van Dijck, D. Geldof, F. Blockhuys, B. Prelot, J. Zajac, V. Meynen, Aqueous or solvent based surface modification: The influence of the combination solvent – organic functional group on the surface characteristics of titanium dioxide grafted with organophosphonic acids, Appl. Surf. Sci. 416 (2016) 716–724. doi:10.1016/j.apsusc.2017.04.143.

[21] A. Roevens, J.G. Van Dijck, M. Tassi, J. D'Haen, R. Carleer, P. Adriaensens, F. Blockhuys, V. Meynen, Revealing the influence of solvent in combinatin with temperature, concentration and pH on the modification of TiO_2 with propylphosphonic acid, Mater. Chem. Phys. 184 (2016) 324–334.

doi:10.1016/j.matchemphys.2016.09.059.

[22] G. Mustafa, Development of an efficient anti-fouling grafting to enhance the applicability of ceramic nanofiltration membranes in water treatment, University of Antwerp, 2016.

[23] G. Mustafa, K. Wyns, A. Buekenhoudt, V. Meynen, New insights into the fouling mechanism of dissolved organic matter applying nanofiltration membranes with a variety of surface chemistries, Water Res. 93 (2016) 195–204. doi:10.1016/j.watres.2016.02.030.

[24] G. Mustafa, K. Wyns, A. Buekenhoudt, V. Meynen, Antifouling grafting of ceramic membranes validated in a variety of challenging wastewaters, Water Res. 104 (2016) 242–253. doi:10.1016/j.watres.2016.07.057.

[25] G. Mustafa, K. Wyns, P. Vandezande, A. Buekenhoudt, V. Meynen, Novel grafting method efficiently decreases irreversible fouling of ceramic nanofiltration membranes, J. Memb. Sci. 470 (2014) 369–377.

[26] S.R. Hosseinabadi, K. Wyns, V. Meynen, R. Carleer, P. Adriaensens, A. Buekenhoudt, B. Van Der Bruggen, Organic solvent nanofiltration with Grignard functionalised ceramic nanofiltration membranes, J. Memb. Sci. 454 (2014) 496–504. doi:10.1016/j.memsci.2013.12.032.

[27] S.R. Hosseinabadi, K. Wyns, V. Meynen, A. Buekenhoudt, B. Van der Bruggen, Solvent-membrane-solute interactions in organic solvent nanofiltration (OSN) for Grignard functionalised ceramic membranes: Explanation via Spiegler-Kedem theory, J. Memb. Sci. 513 (2016) 177–185. doi:10.1016/j.memsci.2016.04.044.

[28] G. Mustafa, K. Wyns, S. Janssens, A. Buekenhoudt, V. Meynen, Evaluation of the fouling resistance of methyl grafted ceramic membranes for inorganic foulants and co-effects of organic foulants, Sep. Purif. Technol. 193 (2018) 29–37. doi:10.1016/j.seppur.2017.11.015.

[29] D. Ormerod, M. Dorbec, E. Merkul, N. Kaval, N. Lefèvre, S. Hostyn, L. Eykens, J. Lievens, S. Sergeyev, B.U.W. Maes, Synthesis of Pd Complexes Containing Tailed NHC Ligands and Their Use in a Semicontinuous Membrane-Assisted Suzuki Cross-Coupling Process, Org. Process Res. Dev. 22 (2018) 1509–1517. doi:10.1021/acs.oprd.8b00273.

[30] J. Wartmann, H. Deuel, Organische Derivate des Silikagels mit Si-C-Bindung II, Helv. Chim. Acta. 42 (1959) 1166–1170.

[31] J. Lim, C. Shim, J. Kim, B.Y. Lee, J.E. Yie, Dehydroxylation route to surface modification of mesoporous silicas by using Grignard reagents, Angew. Chemie Int. Ed. 43 (2004) 3839–3842. doi:10.1002/anie.200454076.

[32] S. Angloher, T. Bein, Organic functionalisation of mesoporous silica, Stud. Surf. Sci. Catal. 158 (2005) 2017–2026. http://www.sciencedirect.com/science/article/pii/S0167299105805683 (accessed July 28, 2014).

[33] S. Angloher, T. Bein, Metalorganic modification of periodic mesoporous silica: aromatic nitrogen functionalities, J. Mater. Chem. 16 (2006) 3629. doi:10.1039/b605283e.

[34] S. Angloher, J. Kecht, T. Bein, Optimization of reaction conditions for the metalorganic modification of MCM-41, Chem. Mater. 109 (2007) 3568–3574. http://pubs.acs.org/doi/abs/10.1021/cm0608387 (accessed August 19, 2014).

[35] J. Kecht, T. Bein, Functionalization of colloidal mesoporous silica by metalorganic

reagents, Langmuir. 24 (2008) 14209–14214. doi:10.1021/la802115n.

[36] S. Angloher, J. Kecht, T. Bein, Mesoporous ordered silica structures modified by metal organic reagents and their application in catalytic Michael additions, Microporous Mesoporous Mater. 115 (2008) 629–633. doi:10.1016/j.micromeso.2008.02.019.

[37] V. Müller, F. Haase, J. Rathousky, D. Fattakhova-Rohlfing, Surface functionalization of mesoporous antimony doped tin oxide by metalorganic reaction, Mater. Chem. Phys. 137 (2012) 207–212. doi:10.1016/j.matchemphys.2012.09.008.

[38] N.Y. Kim, P.E. Laibinis, Improved polypyrrole/silicon junctions by surfacial modification of hydrogen-terminated silicon using organolithium reagents, J. Am. Chem. Soc. 121 (1999) 7162–7163. doi:10.1021/ja990260k.

[39] N.Y. Kim, P.E. Laibinis, Derivitization of porous silicon by grignard reagents at room temperatue, J.Am Chem Soc. 120 (1998) 4516–4517.

[40] J.H. Song, M.J. Sailor, Functionalization of nanocrystalline porous silicon surfaces with aryllithium reagnets: Formation of silicon-carbon bonds by cleavage of silicon-silicon bonds, J. Am. Chem. Soc. 120 (1998) 2376–2381. doi:10.1021/ja9734511.

[41] R. Boukherroub, S. Morin, F. Bensebaa, D.D.M. Wayner, New synthetic routes to alkyl monolayers on the Si(111) surface, Langmuir. 15 (1999) 3831–3835. doi:10.1021/la9901478.

[42] D.D.M. Wayner, R.A. Wolkow, Organic modification of hydrogen terminated silicon surfaces, J. Chem. Soc. Perkin Trans. 2. 1 (2002) 23–34. doi:10.1039/b100704l.

[43] A. Buekenhoudt, K. Wyns, V. Meynen, B. Maes, P. Cool, Surface-modified inorganic matrix and method for preparation thereof, WO 2010/106167, 2010.

[44] P. Van Heetvelde, E. Beyers, K. Wyns, P. Adriaensens, B.U.W. Maes, S. Mullens, A. Buekenhoudt, V. Meynen, A new method to graft titania using Grignard, Chem. Commun. 49 (2013) 6998–7000. doi:10.1039/c3cc43695k.

[45] L. Bin Xiong, J.L. Li, B. Yang, Y. Yu, Ti^{3+} in the surface of titanium dioxide: Generation, properties and photocatalytic application, J. Nanomater. (2012). doi:10.1155/2012/831524.

[46] X. Yan, Y. Li, T. Xia, Black Titanium Dioxide Nanomaterials in Photocatalysis, Int. J. Photoenergy. (2017). doi:10.1155/2017/8529851.

[47] J. Xu, Z. Tian, G. Yin, T. Lin, F. Huang, Controllable reduced black titania with enhanced photoelectrochemical water splitting performance, Dalt. Trans. 46 (2017) 1047–1051. doi:10.1039/C6DT04060H.

[48] X. Liu, G. Zhu, X. Wang, X. Yuan, T. Lin, F. Huang, Progress in Black Titania: A New Material for Advanced Photocatalysis, Adv. Energy Mater. 6 (2016) 1–29. doi:10.1002/aenm.201600452.

[49] T. Van Gestel, C. Vandecasteele, A. Buekenhoudt, C. Dotremont, J. Luyten, R. Leysen, B. Van Der Bruggen, G. Maes, Salt retention in nanofiltration with multilayer ceramic TiO_2 membranes, J. Memb. Sci. 209 (2002) 379–389. doi:10.1016/S0376-7388(02)00311-3.

[50] S. Shamaila, A.K. Leghari Sajjad, F. Chen, J. Zhang, Mesoporous titania with high crystallinity during synthesis by dual template system as an efficient photocatalyst, Catal. Today. 175 (2011) 568–575. doi:10.1016/j.cattod.2011.03.041.

[51] S. Loreto, H. Vanrompay, M. Mertens, S. Bals, V. Meynen, The Influence of Acids on Tuning the Pore Size of Mesoporous TiO_2 Templated by Non-Ionic Block Copolymers, Eur. J. Inorg. Chem. 2018 (2018) 62–65. doi:10.1002/ejic.201701266.

[52] J. Verbeeck, S. Van Aert, Model based quantification of EELS spectra, Ultramicroscopy. 101 (2004) 207–224. doi:10.1016/j.ultramic.2004.06.004.

[53] A. Krasovskiy, P. Knochel, Convenient titration method for organometallic zinc, magnesium, and lanthanide reagents, Synthesis (Stuttg). (2006) 890–891. doi:10.1055/s-2006-926345.

[54] K. Yamamoto, T. Tatsumi, Organic functionalization of mesoporous molecular sieves with Grignard reagents, Microporous Mesoporous Mater. 44–45 (2001) 459–464. http://www.sciencedirect.com/science/article/pii/S1387181101002219 (accessed July 28, 2014).

[55] G. Dong, X. Wang, Z. Chen, Z. Lu, Enhanced Photocatalytic Activity of Vacuum-activated TiO_2 Induced by Oxygen Vacancies, Photochem. Photobiol. 94 (2018) 472–483. doi:10.1111/php.12874.

[56] G. Socrates, Infrared and Raman characteristic group frequencies, 2004. doi:10.1002/jrs.1238.

[57] C. Morterra, An infrared spectroscopic study of anatase properties. Part 6. - Surface hydration and strong Lewis acidity of pure and sulphate-doped preparations, J. Chem. Soc. Faraday Trans. 1. 84 (1988) 1617. doi:10.1039/f19888401617.

[58] G. Martra, Lewis acid and base sites at the surface of microcrystalline $TiO_2$2 anatase: relationships between surface morphology and chemical behaviour, Appl. Catal. A Gen. 200 (2000) 275–285. doi:10.1016/S0926-860X(00)00641-4.

[59] D. Yates, Infrared studies of the surface hydroxyl groups on titanium dioxide, and of the chemisorption of carbon monoxide and carbon dioxide, J. Phys. Chem. 65 (1961) 746–753. http://pubs.acs.org/doi/abs/10.1021/j100823a011 (accessed October 6, 2014).

[60] S. Pletincx, J.M.C. Mol, H. Terryn, A. Hubin, T. Hauffman, An in situ spectro-electrochemical monitoring of aqueous effects on polymer/metal oxide interfaces, J. Electroanal. Chem. 848 (2019) 113311. doi:10.1016/j.jelechem.2019.113311.

[61] G. Busca, H. Saussey, O. Saur, J.C. Lavalley, V. Lorenzelli, FT-IR characterization of the surface acidity of different titanium dioxide anatase preparations, Appl. Catal. 14 (1985) 245–260. doi:10.1016/S0166-9834(00)84358-4.

[62] H. Lin, J. Long, Q. Gu, W. Zhang, R. Ruan, Z. Li, X. Wang, In situ IR study of surface hydroxyl species of dehydrated TiO_2: Towards understanding pivotal surface processes of TiO_2 photocatalytic oxidation of toluene, Phys. Chem. Chem. Phys. 14 (2012) 9468–9474. doi:10.1039/c2cp40893g.

[63] Y. Bouvier, B. Mutel, J. Grimblot, Use of an Auger parameter for characterizing the Mg chemical state in different materials, Surf. Coatings Technol. 180–181 (2004) 169–173. doi:10.1016/j.surfcoat.2003.10.062.

[64] S. Ardizzone, C.L. Bianchi, M. Fadoni, B. Vercelli, Magnesium salts and oxide: An XPS overview, Appl. Surf. Sci. 119 (1997) 253–259. doi:10.1016/S0169-4332(97)00180-3.

[65] E. Morra, E. Giamello, M. Chiesa, EPR approaches to heterogeneous catalysis. The chemistry of titanium in heterogeneous catalysts and photocatalysts, J. Magn. Reson. 280 (2017) 89–102.

[66] M. Wesolowski, E. Leyk, P. Szynkaruk, Detection of magnesium compounds in dietary supplements and medicinal products by DSC, Infrared and Raman techniques, J. Therm. Anal. Calorim. 116 (2014) 671–680. doi:10.1007/s10973-014-3762-y.

[67] K.O. Akira Ookubo, Eiji Kanezaki, ESR, XRD, and DRS Studies of Paramagnetic Ti^{3+} Ions in a.pdf, (1989) 206–209.

[68] C. Kormann, D.W. Bahnemann, M.R. Hoffmann, Preparation and characterization of

quantum-size titanium dioxide, J. Phys. Chem. 92 (1988) 5196–5201. doi:10.1021/j100329a027.

[69] M.S. Hamdy, R. Amrollahi, G. Mul, activity and selectivity in visible light stimulated selective oxidation Surface Ti^{3+} containing (blue) titania : A unique photocatalyst with high activity and selectivity in visible light stimulated selective oxidation, ACS Catal. 2 (2012) 2641–2647. doi:dx.doi.org/10.1021/cs300593d.

[70] B. Ohtani, Y. Ogawa, S. Nishimoto, Photocatalytic Activity of Amorphous-Anatase Mixture of Titanium(IV) Oxide Particles Suspended in Aqueous Solutions Bunsho, J. Phys. Chem. B. 101 (1997) 3746–3752.

[71] E. Matijević, M. Budnik, L. Meites, Preparation and mechanism of formation of titanium dioxide hydrosols of narrow size distribution, J. Colloid Interface Sci. 61 (1977) 302–311. doi:10.1016/0021-9797(77)90393-9.

[72] S.K. Samantaray, P. Mohapatra, K. Parida, Physico-chemical characterisation and photocatalytic activity of nanosized SO_4^{2-}/TiO_2 towards degradation of 4-nitrophenol, J. Mol. Catal. A Chem. 198 (2003) 277–287. doi:10.1016/S1381-1169(02)00693-3.

[73] M. Yan, F. Chen, J. Zhang, M. Anpo, Preparation of controllable crystalline titania and study on the photocatalytic properties, J. Phys. Chem. B. 109 (2005) 8673–8678. doi:10.1021/jp046087i.

[74] C. Liu, L. Fu, J. Economy, A simple, template-free route for the synthesis of mesoporous titanium dioxide materials, J. Mater. Chem. 14 (2004) 1187–1189. doi:10.1039/b316426h.

[75] A. Zaban, S.T. Aruna, S. Tirosh, B.A. Gregg, Y. Mastai, The Effect of the Preparation Condition of TiO_2 Colloids on Their Surface Structures, J. Phys. Chem. B. 104 (2000) 4130–4133. doi:10.1021/jp993198m.

Figure Captions

Figure 1: IR spectra at 150 °C under vacuum of unmodified fresh P25 (a), unmodified P25 after vacuum treatment (b), P25 blank sample (c), P25 modified with ethylmagnesium bromide (d), P25 modified with n-propylmagnesium chloride (e) and P25 modified with octylmagnesium chloride (f). A: region 3900 cm^{-1} to 2600 cm^{-1}, B: region 1900 cm^{-1} to 900 cm^{-1}

Figure 2: Survey(A) and multiplex (B) of unmodified P25 (black), P25 modified with ethylmagnesium bromide after full washing (red) and P25 modified with ethylmagnesium bromide after THF washing step(green).

Figure 3: Mg2s signal measured by XPS for a P25 sample modified with ethylmagnesium bromide after the first washing step.

*Figure 4: EPR measurement recorded at 25 K and RT of P25 modified with ethylmagnesium bromide(ethyl) and with octylmagnesium chloride (octyl). * indicates signal due to copper contamination.*

Figure 5: TGA(dotted, right axis) and DTG(full, left axis) of P25 modified samples with different amounts of octylmagnesium chloride.

Figure 6: IR spectra at 150 °C under vacuum of P25 modified with different amounts of octylmagnesium chloride measured at 150 °C under vacuum: unmodified P25 after vacuum treatment (a), 2mmol (b), 3mmol (c), 4mmol (d), 6mmol (e), 6 mmol after extra wash (f). A: region 3900 cm^{-1} to 2600 cm^{-1}, B: region 1900 cm^{-1} to 900 cm^{-1}

Figure 7: Overlay O1s & Mg2s signal (normalized) measured by XPS for P25 modified with ethylmagnesium bromide after the first washing step. (black) and P25 modified with 6 mmol octylmagnesium choride (red)

Figure 8: XPS Multiplex of P25 modified with 6mmol octylmagnesium chloride (red) and the same sample after extra washing (black).

Figure 9: TGA(dotted, right axis) and DTG (full, left axis) of octylmagnesium chloride modified samples at different reaction times and an unmodified P25 sample

Figure 10: Percentage of Grignard reactant left after 4 h, 24 h, 48 h and 72 h for the modification of P25 with propylmagnesium chloride or octylmagnesium chloride. The percentage was determined by the titration method described in 2.4

Figure 11: EPR measurement recorded at RT and 25K of P25 modified with octylmagnesium chloride at RT and at 65 °C.

Figure 12: TGA(dotted, right axis) and DTG(full, left axis) of P25 modified with octylmagnesium chloride samples at different temperatures and times and an unmodified P25.

Figure 13: IR spectra of P25 modified with octylmagnesium chloride at different reaction temperatures and times measured at 150 °C under vacuum: unmodified P25 after vacuum treatment (a), 4h at RT (b), 4h at 65 °C (c), 4h at -78 °C (d), 24h at RT (e), 24h at 65 °C (f) and 24h started at -78 °C (g). A: region 3900 cm^{-1} to 2600 cm^{-1}, B: region 1900 cm^{-1} to 900 cm^{-1}

Figure 14: DTG curves of different (modified) titania supports. P25 (a), PC500 (b), TiO_2 HCl (c), TiO_2 H_2SO_4-1(d), $sTiO_2$ (e), TiO_2 H_2SO_4-0.1 (f), TiO_2 H_2SO_4-0.01 (g).Purple curve is the unmodified support, blue curve is the support modified with octylmagnesium chloride.

Figure 15: EPR measurement recorded at RT and 25 K of $sTiO_2$ modified with ethylmagnesium bromide(ethyl) and with octylmagnesium chloride (octyl). The broad features observed in the low-temperature EPR spectrum of the ethyl case are likely to originate from small amounts of Fe(III) contaminants.

Figure 16: TGA(dotted, right axis) and DTG(full, left axis) of $sTiO_2$ modified samples with different amounts of octylmagnesium chloride.

Figure 17: IR spectra of $sTiO_2$ modified with different amounts of octylmagnesium chloride measured at 150 °C under vacuum: unmodified $sTiO_2$ after vacuum treatment (a), 2 mmol (b), 3 mmol (c), 4 mmol after extra wash (d), 6 mmol after extra wash (e). A: region 3900 cm^{-1} to 2600 cm^{-1}, B: region 1900 cm^{-1} to 900 cm^{-1}

Figure 18: TGA(dotted, right axis) and DTG(full, left axis) of 8Gr modified samples with different reaction times and an unmodified $sTiO_2$ sample.

Figure 19: EPR measurement recorded at RT and 25K of TiO_2 modified with octylmagnesium chloride at RT and at 65 °C. The broad features observed in the low-temperature EPR spectrum of the titania modified at 65 °C are likely to originate from small amounts of Fe(III)-containing contaminants.

Figure 20: TGA and DTG of octylmagnesium chloride modified samples at different temperatures and times and an unmodified $sTiO_2$ sample.

Figure 21: IR spectra of $sTiO_2$ modified with octylmagnesium chloride at different reaction temperatures and times measured at 150 °C under vacuum: unmodified $sTiO_2$ after vacuum treatment (a), 4 h at RT (b), 4 h at 65 °C (c), 4 h at -78 °C (d), 24 h at RT (e), 24 h at 65 °C (f) and 24 h started at -78 °C (g). A: region 3900 cm^{-1} to 2600 cm^{-1}, B: region 1900 cm^{-1} to 900 cm^{-1}

Figures

Fig.1

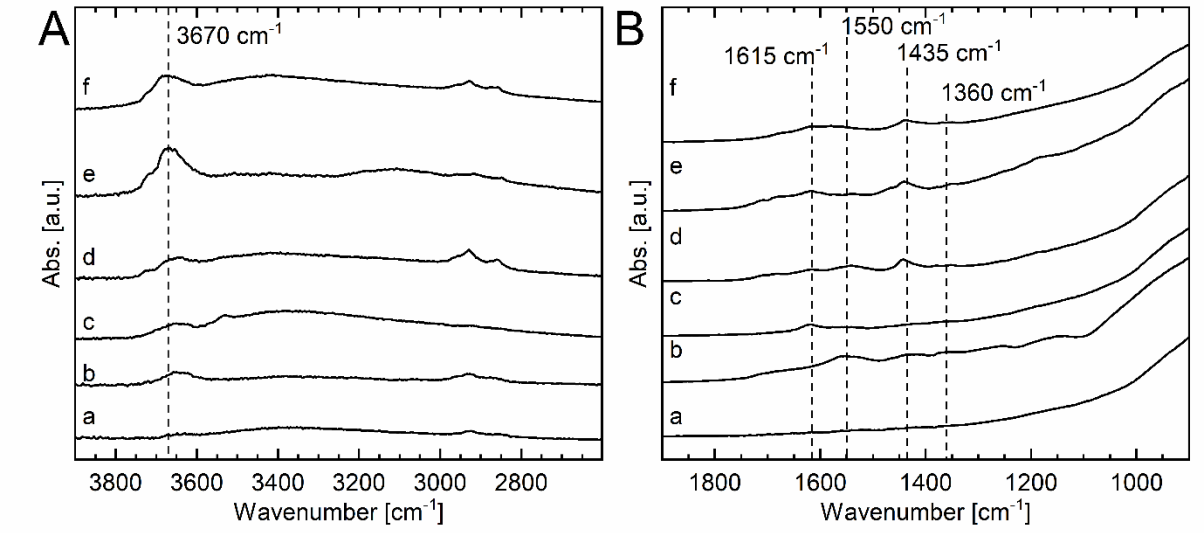

Fig. 2

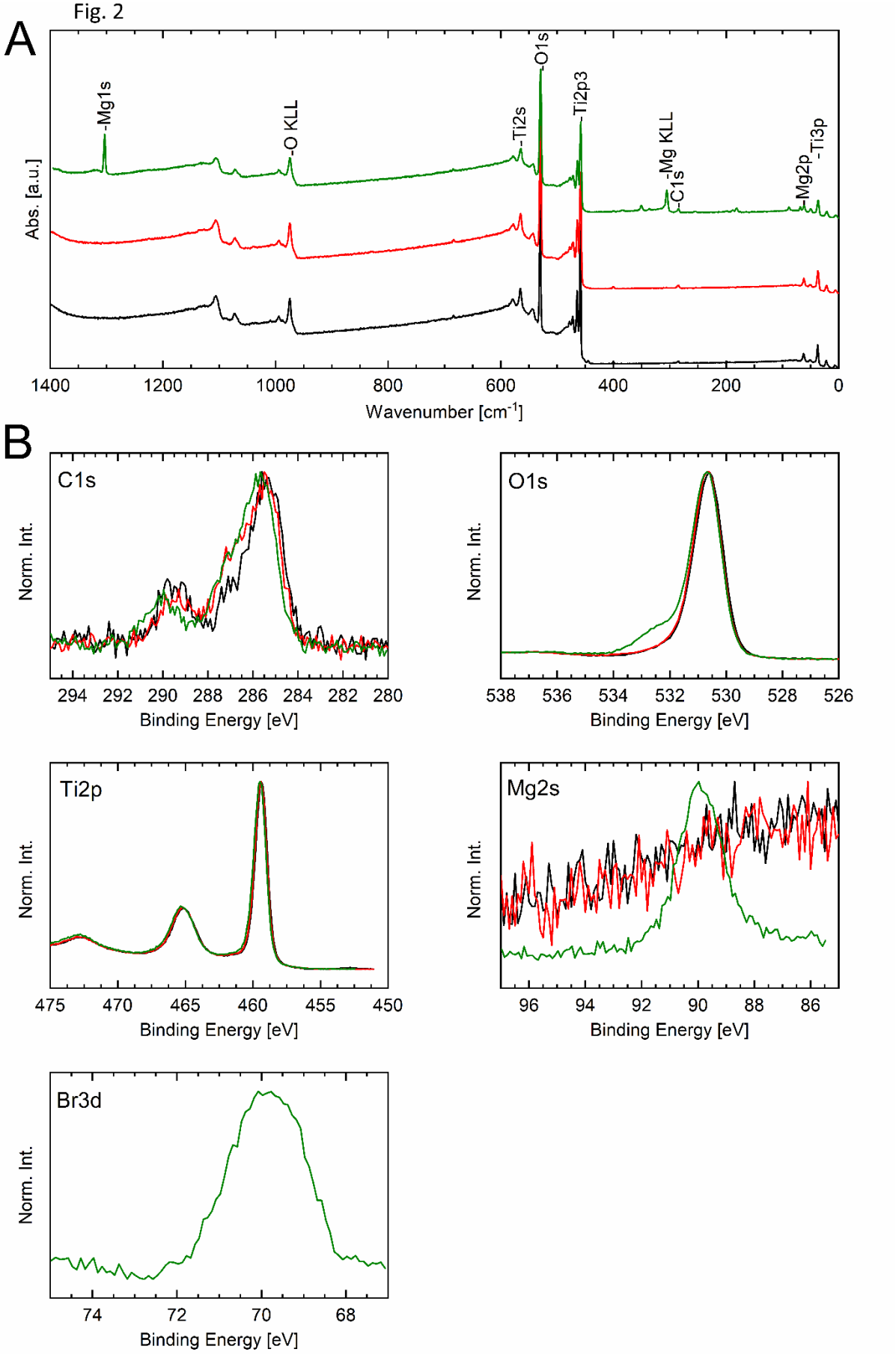
A
Mg1s
O KLL
Ti2s
O1s
Ti2p3
Mg KLL
C1s
Mg2p
Ti3p
Abs. [a.u.]
1400
1200
1000
800
600
400
200
0
Wavenumber [cm-1]
B
C1s
Norm. Int.
294 292 290 288 286 284 282 280
Binding Energy [eV]
O1s
Norm. Int.
538 536 534 532 530 528 526
Binding Energy [eV]
Ti2p
Norm. Int.
475 470 465 460 455 450
Binding Energy [eV]
Mg2s
Norm. Int.
96 94 92 90 88 86
Binding Energy [eV]
Br3d
Norm. Int.
74 72 70 68
Binding Energy [eV]

Fig. 3

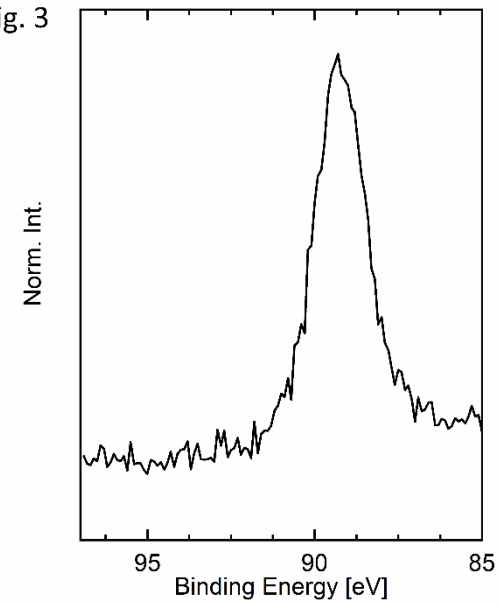
Norm. Int.
95
90
85
Binding Energy [eV]

Fig. 4

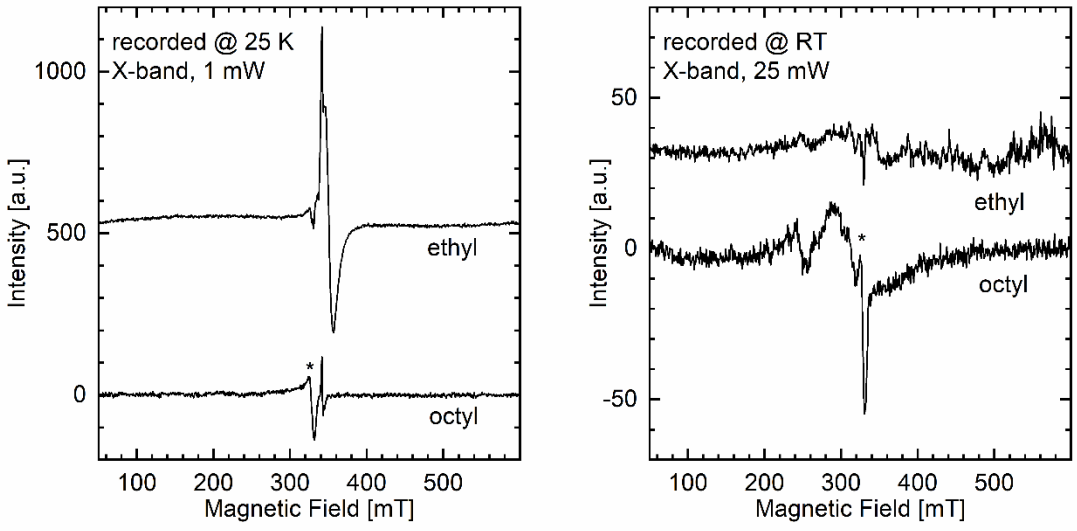
recorded @ 25 K
X-band, 1 mW
1000
500
0
Intensity [a.u.]
ethyl
octyl
*
100
200
300
400
500
Magnetic Field [mT]
recorded @ RT
X-band, 25 mW
50
0
-50
Intensity [a.u.]
ethyl
octyl
*
100
200
300
400
500
Magnetic Field [mT]

Fig. 5

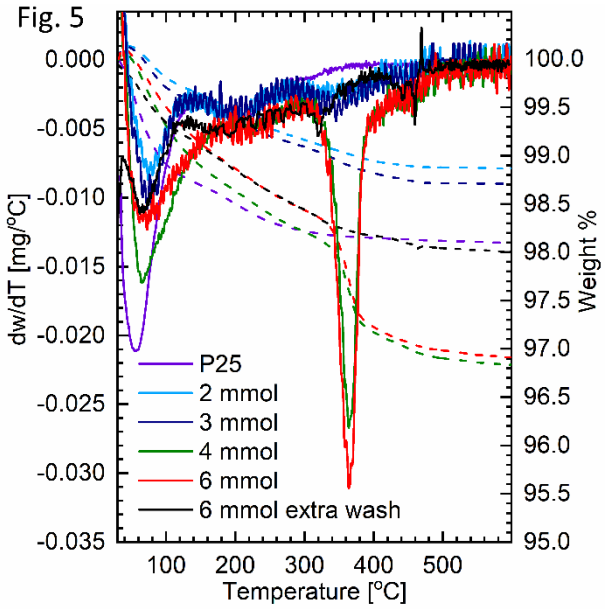
dw/dT [mg/°C]
Weight %
Temperature [°C]
P25
2 mmol
3 mmol
4 mmol
6 mmol
6 mmol extra wash

Fig. 6

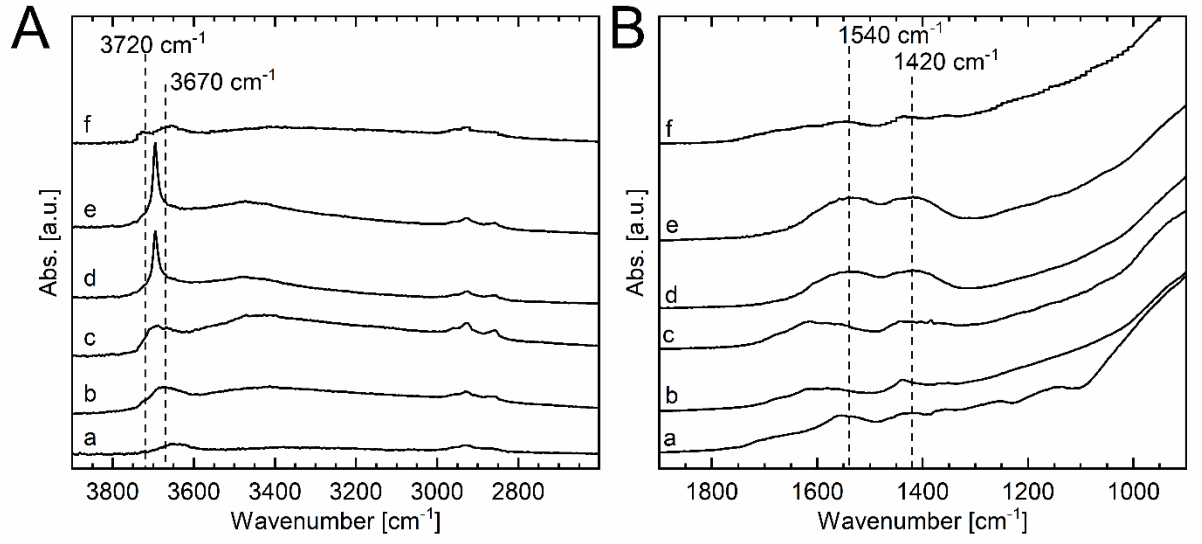
A
3720 cm-1
3670 cm-1
Abs. [a.u.]
Wavenumber [cm-1]
B
1540 cm-1
1420 cm-1
Abs. [a.u.]
Wavenumber [cm-1]

Fig. 7

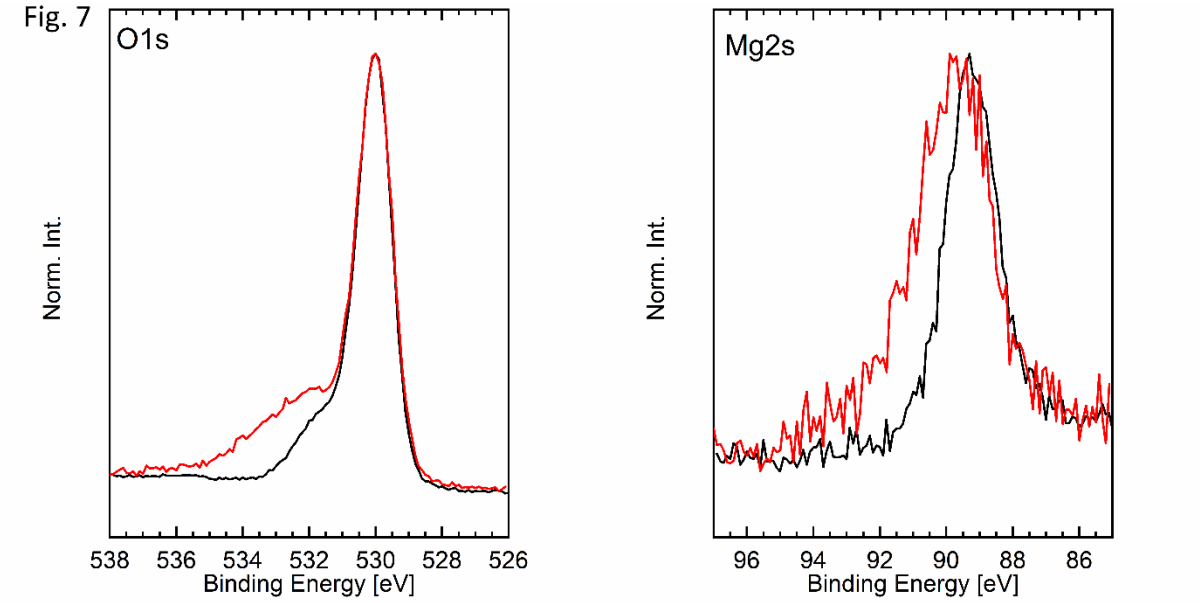
O1s
Norm. Int.
538
536
534
532
530
528
526
Binding Energy [eV]
Mg2s
Norm. Int.
96
94
92
90
88
86
Binding Energy [eV]

Fig. 8

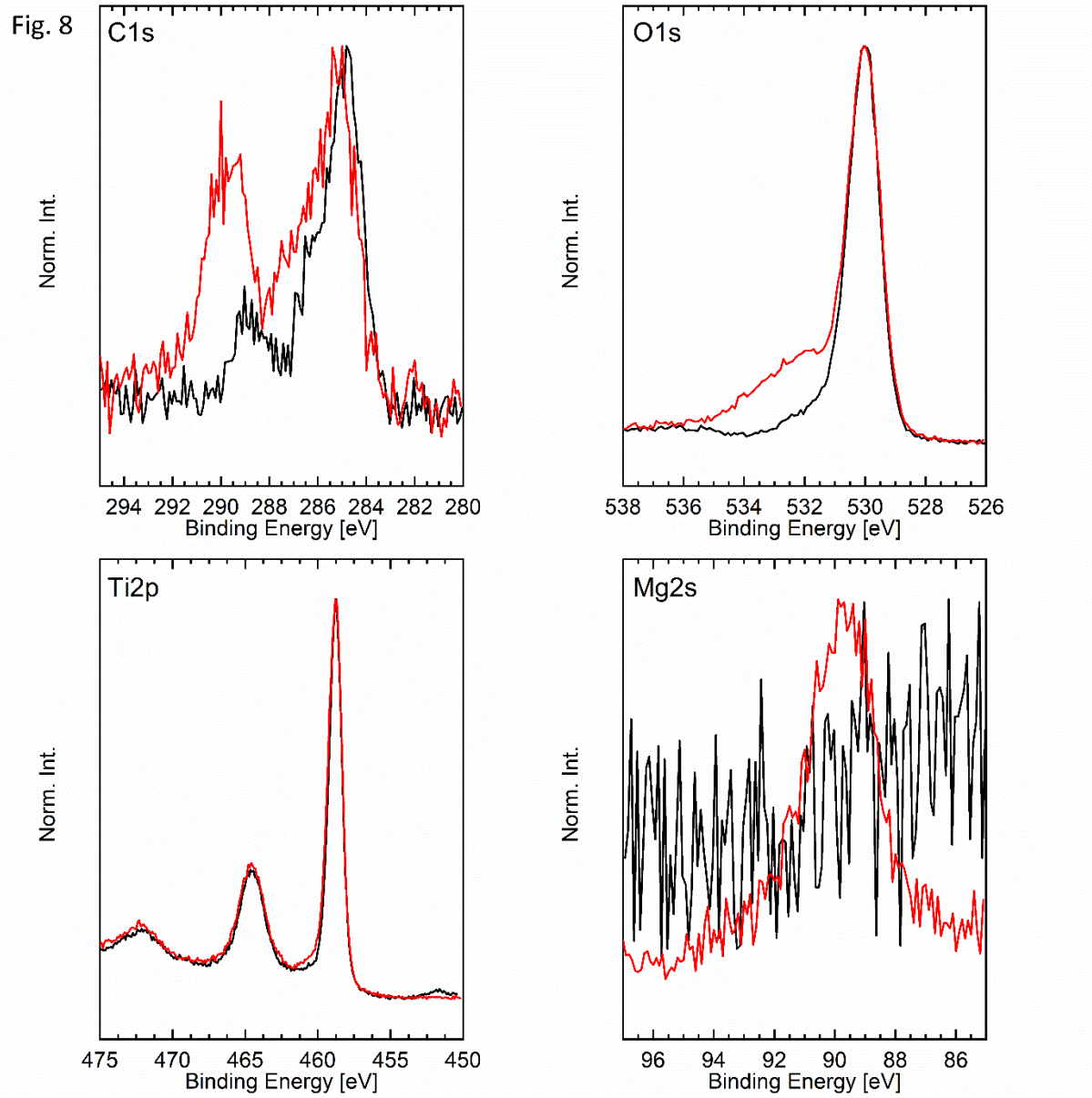
C1s
Norm. Int.
294 292 290 288 286 284 282 280
Binding Energy [eV]
O1s
Norm. Int.
538 536 534 532 530 528 526
Binding Energy [eV]
Ti2p
Norm. Int.
475 470 465 460 455 450
Binding Energy [eV]
Mg2s
Norm. Int.
96 94 92 90 88 86
Binding Energy [eV]

Fig. 9

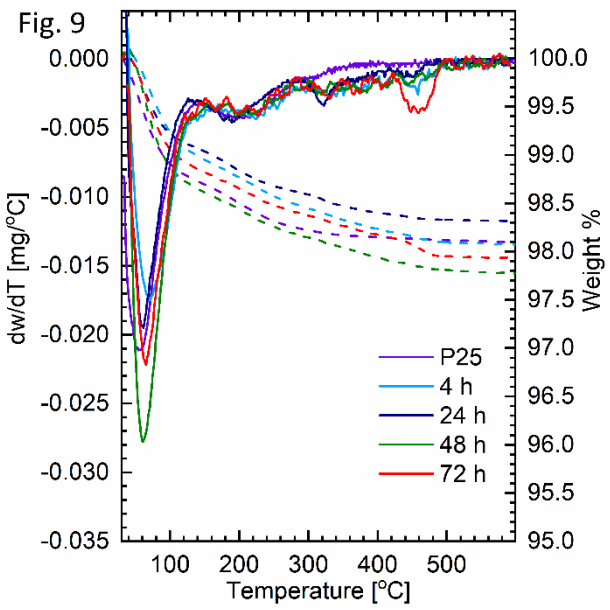
dw/dT [mg/°C]
Weight %
Temperature [°C]
P25
4 h
24 h
48 h
72 h

Fig. 10

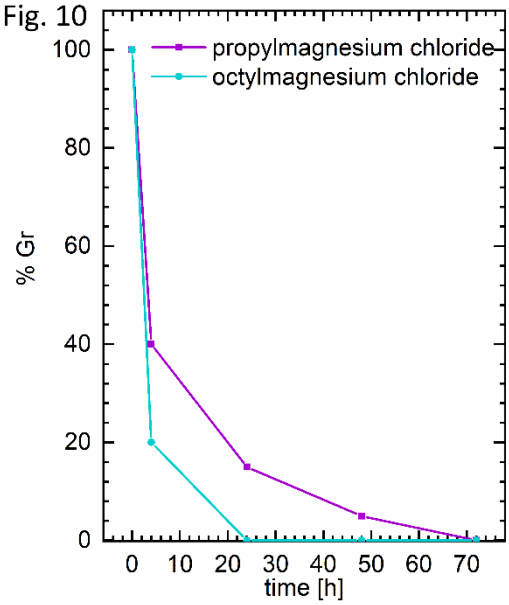
propylmagnesium chloride
octylmagnesium chloride
% Gr
time [h]

Fig. 11

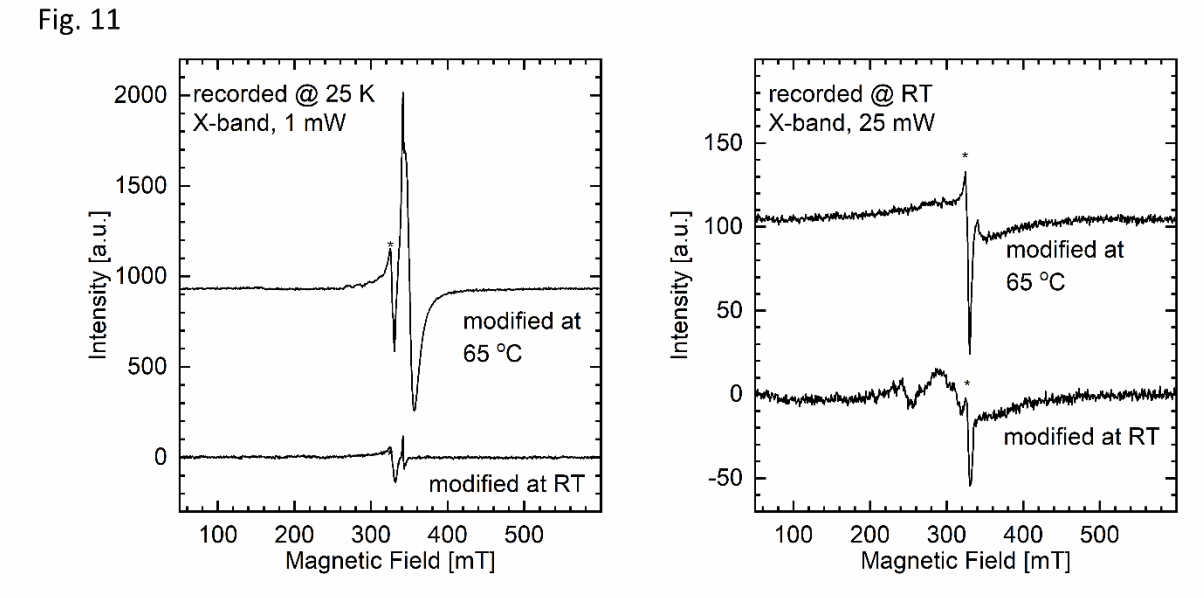
recorded @ 25 K
X-band, 1 mW
modified at
65 °C
modified at RT
Intensity [a.u.]
Magnetic Field [mT]
recorded @ RT
X-band, 25 mW
modified at
65 °C
modified at RT
Intensity [a.u.]
Magnetic Field [mT]

Fig. 12

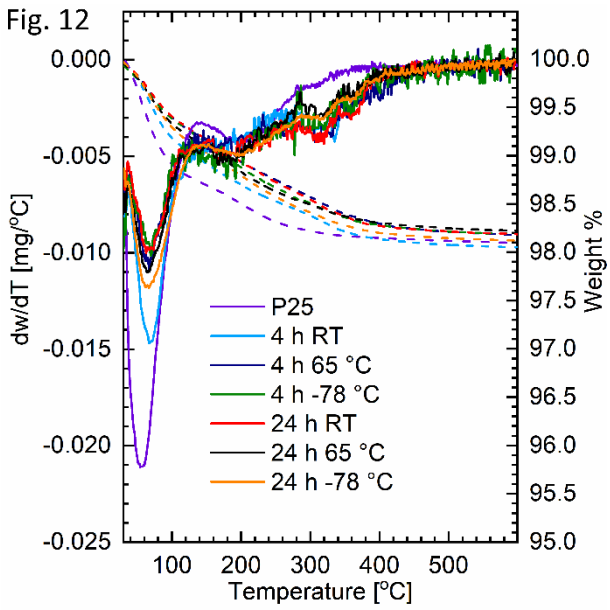
P25
4 h RT
4 h 65 °C
4 h -78 °C
24 h RT
24 h 65 °C
24 h -78 °C
dw/dT [mg/°C]
Weight %
Temperature [°C]

Fig. 13

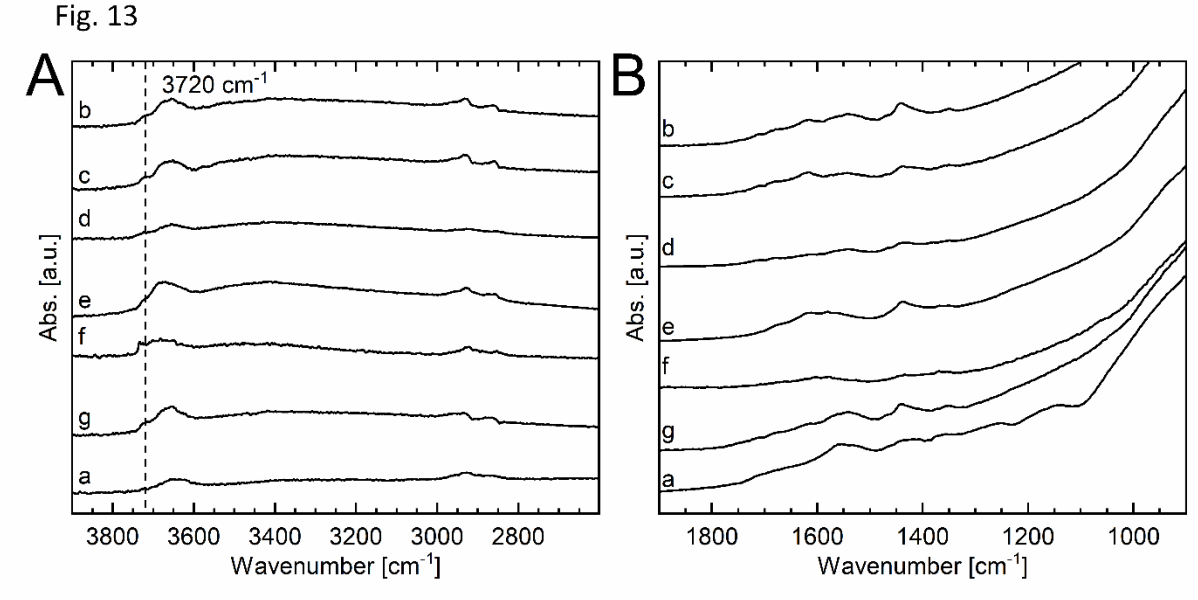
A
3720 cm-1
b
c
d
e
f
g
a
Abs. [a.u.]
3800 3600 3400 3200 3000 2800
Wavenumber [cm-1]
B
b
c
d
e
f
g
a
Abs. [a.u.]
1800 1600 1400 1200 1000
Wavenumber [cm-1]

Fig. 14

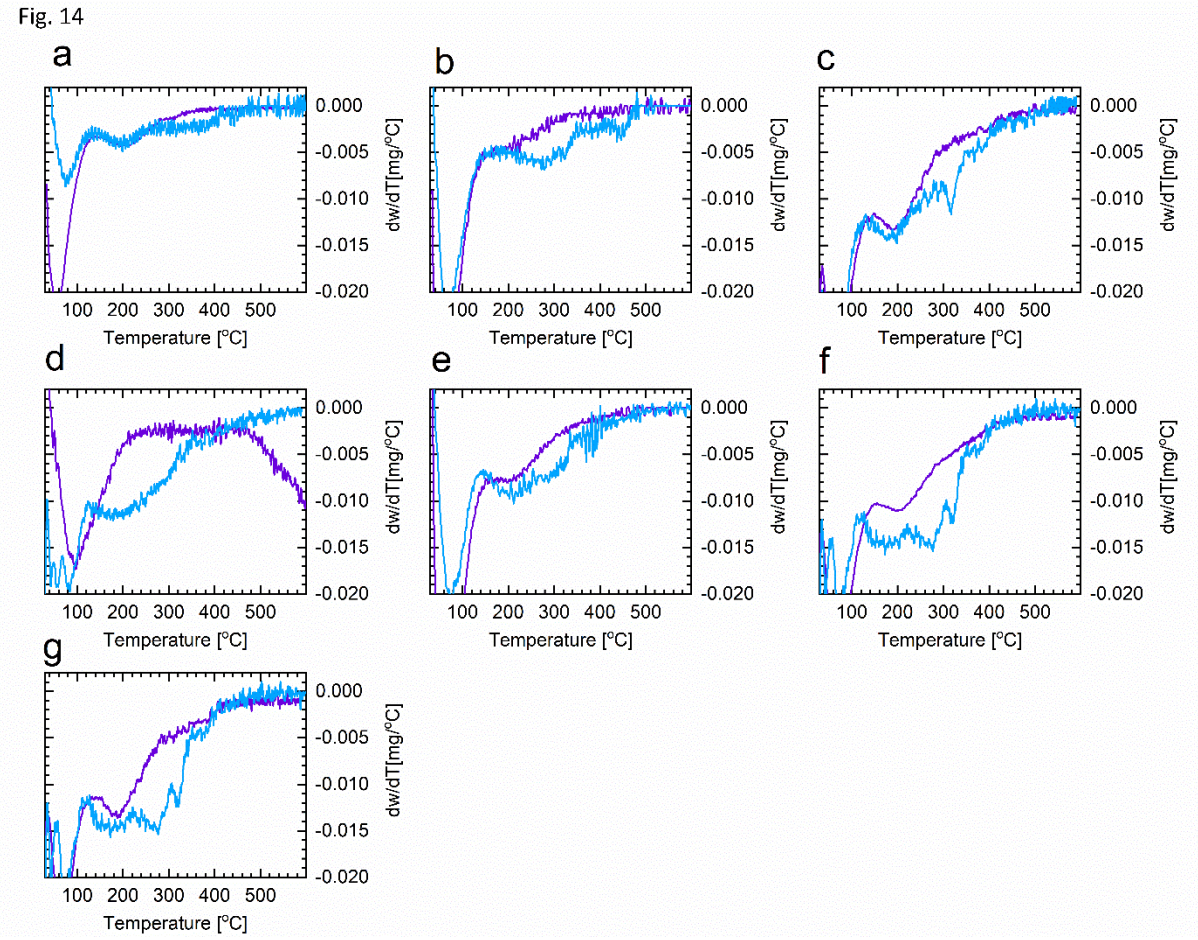
a
b
c
d
e
f
g
0.000
-0.005
-0.010
-0.015
-0.020
dw/dT[mg/°C]
100 200 300 400 500
Temperature [°C]

Fig. 15

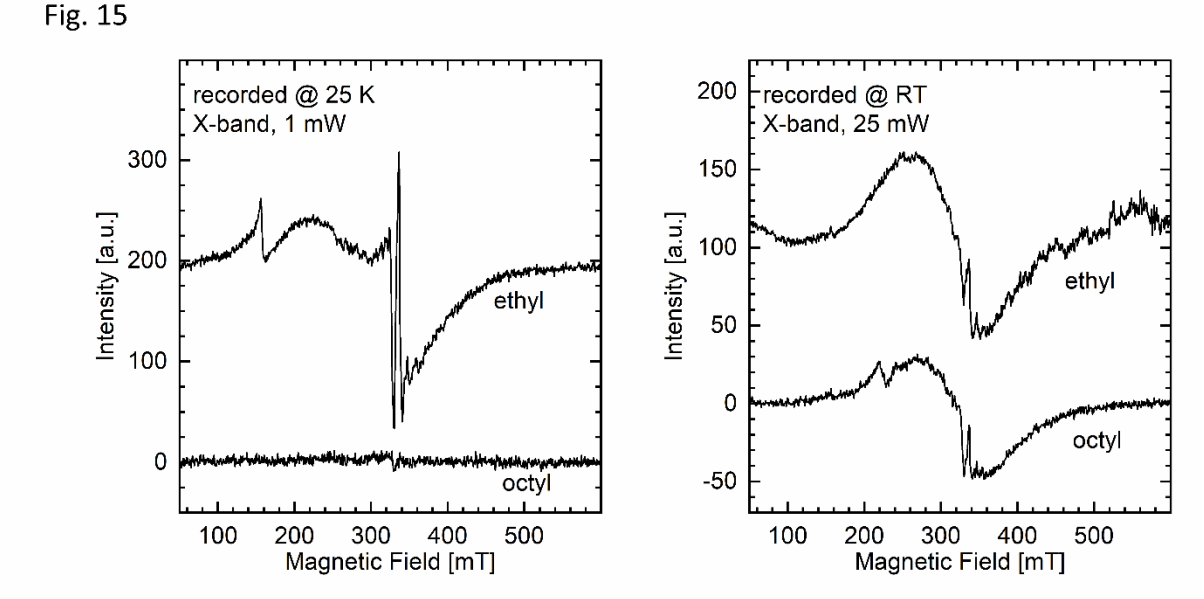
recorded @ 25 K
X-band, 1 mW
Intensity [a.u.]
Magnetic Field [mT]
ethyl
octyl
recorded @ RT
X-band, 25 mW
Intensity [a.u.]
Magnetic Field [mT]
ethyl
octyl

Fig. 16

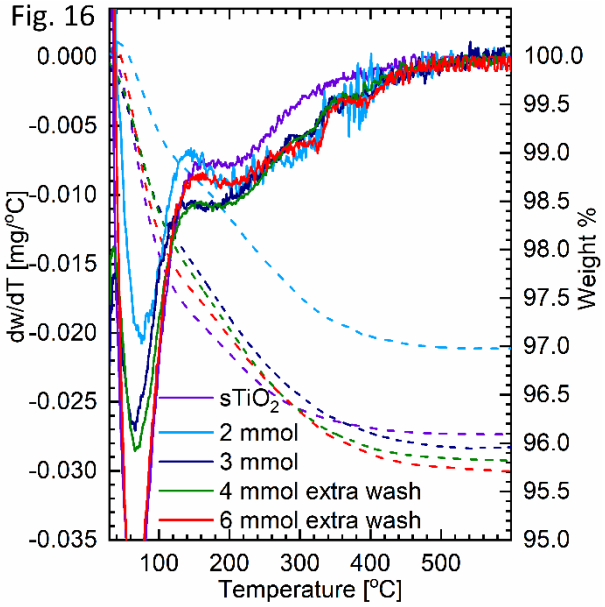
dw/dT [mg/°C]
Weight %
Temperature [°C]
sTiO2
2 mmol
3 mmol
4 mmol extra wash
6 mmol extra wash

Fig. 17

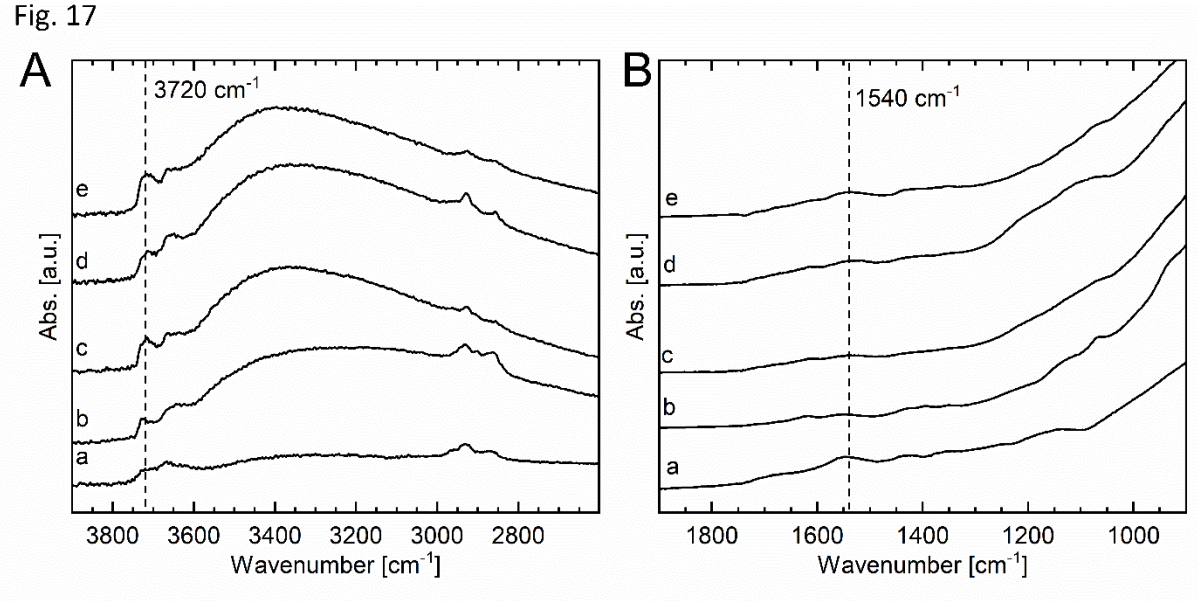
A
3720 cm-1
e
d
c
b
a
Abs. [a.u.]
3800 3600 3400 3200 3000 2800
Wavenumber [cm-1]
B
1540 cm-1
e
d
c
b
a
Abs. [a.u.]
1800 1600 1400 1200 1000
Wavenumber [cm-1]

Fig. 18

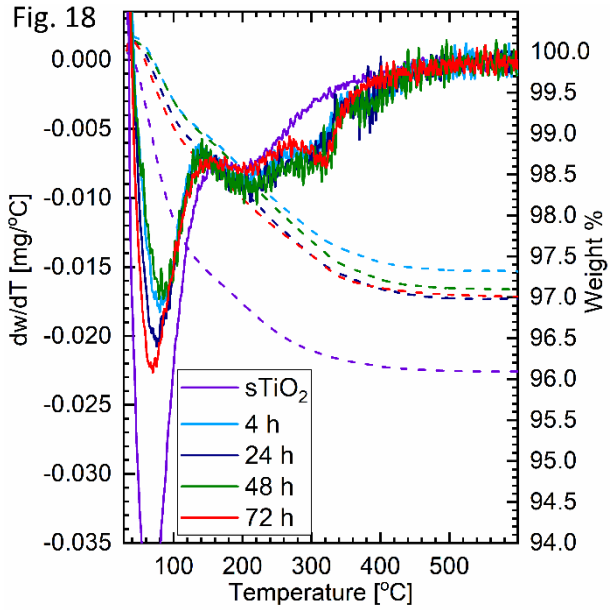
0.000
-0.005
-0.010
-0.015
-0.020
-0.025
-0.030
-0.035
dw/dT [mg/°C]
100.0
99.5
99.0
98.5
98.0
97.5
97.0
96.5
96.0
95.5
95.0
94.5
94.0
Weight %
sTiO2
4 h
24 h
48 h
72 h
100 200 300 400 500
Temperature [°C]

Fig. 19

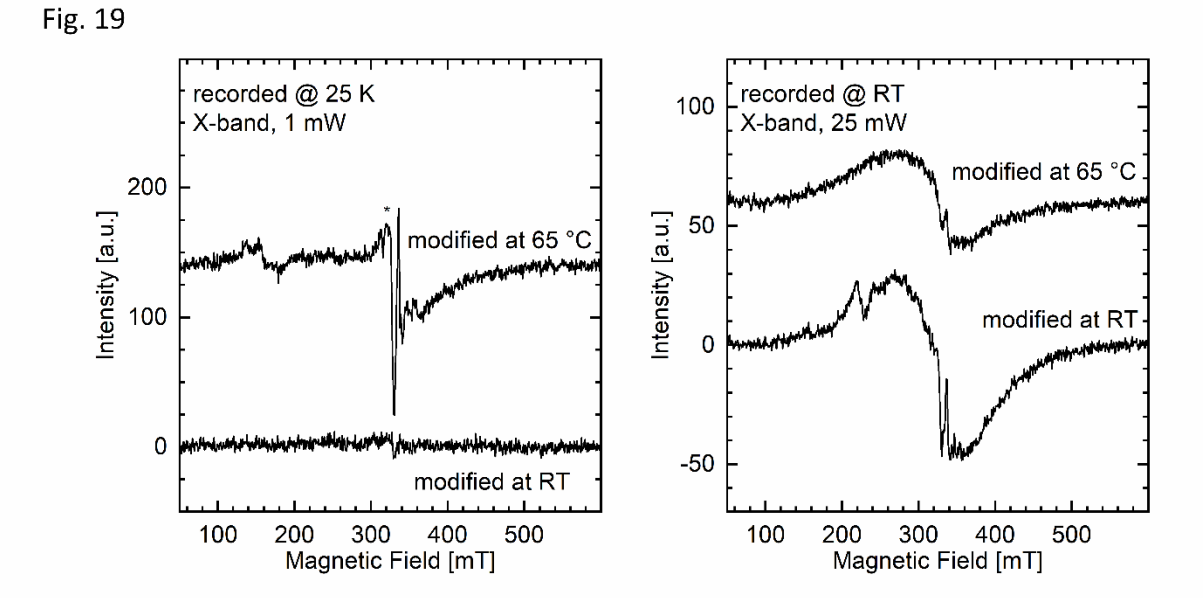
recorded @ 25 K
X-band, 1 mW
modified at 65 °C
modified at RT
Intensity [a.u.]
Magnetic Field [mT]
recorded @ RT
X-band, 25 mW
modified at 65 °C
modified at RT
Intensity [a.u.]
Magnetic Field [mT]

Fig. 20

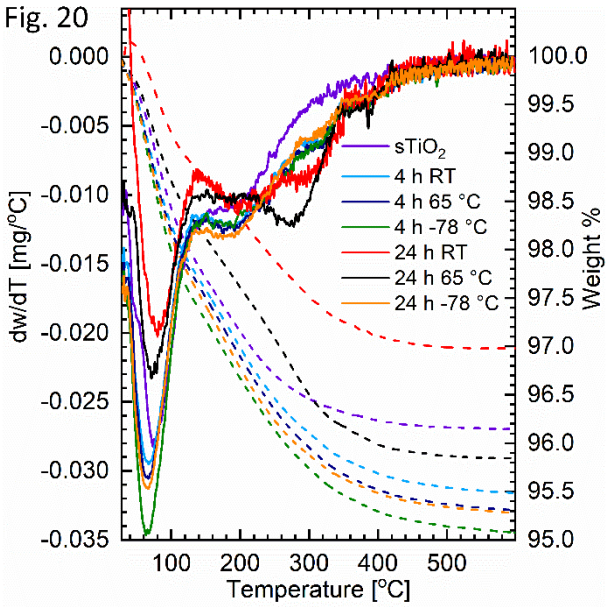
sTiO2
4 h RT
4 h 65 °C
4 h -78 °C
24 h RT
24 h 65 °C
24 h -78 °C
dw/dT [mg/°C]
Weight %
Temperature [°C]

Fig. 21

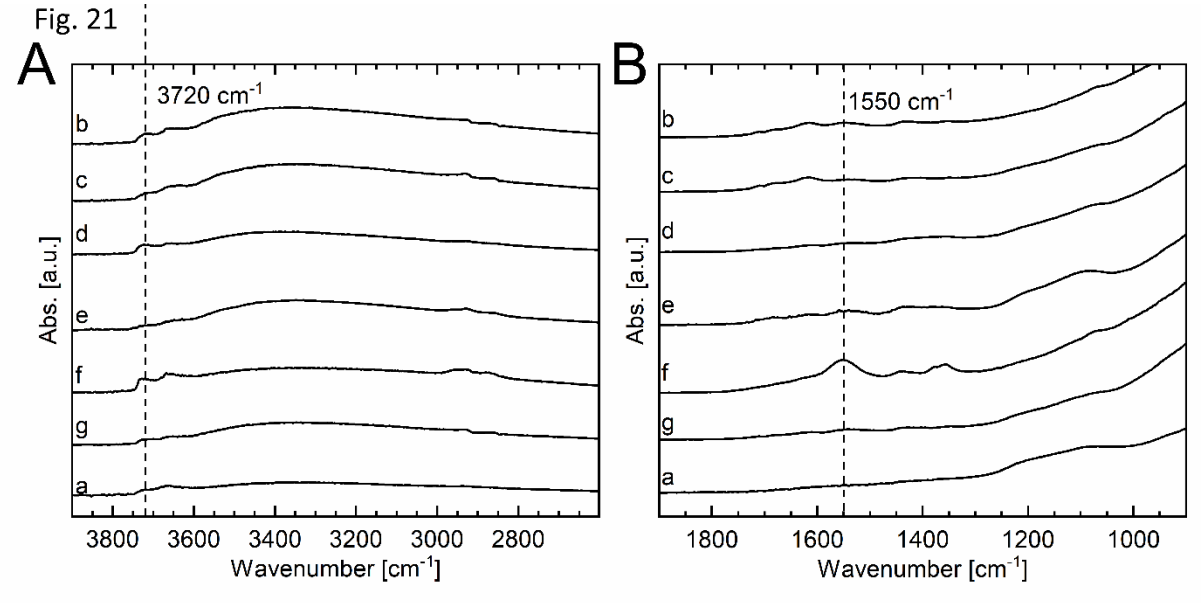
A
3720 cm-1
b
c
d
e
f
g
a
Abs. [a.u.]
3800
3600
3400
3200
3000
2800
Wavenumber [cm-1]
B
1550 cm-1
b
c
d
e
f
g
a
Abs. [a.u.]
1800
1600
1400
1200
1000
Wavenumber [cm-1]